

A numerical modelling of the magnetically insulated diode. Part I: Numerical analysis of the limit problem*

Eugene V. Dulov¹, Pierre Degond², and Alexandre V. Sinityn³

ABSTRACT. We consider a modelling problem of the plane vacuum diode in the magnetic field in the statement by N. Ben Abdallah, P. Degond and F. M'ehats [3]. This problem was finally set by a physicist in late 80-th and was attentively studied by a number of the mathematicians in 90-th. Up to this moment the parameter dependent boundary PDE system has been partially investigated mainly in qualitative aspects. No one complete numerical modelling experiments were made.

In this paper we consider the initial modelling step dealing with a limit problem of the general PDE system, making the bidimensional parameter dependent boundary ODE system. Since the equation system is singular at initial point $t = 0$ and coincide with Gear's definition of stiff ODE system we proposed a combined approach for solving the boundary problem and estimation of parameters, complying the given boundary condition. To do this we use some newly developed derivative free self convergent methods, which proved themselves to be more numerically stable than a classical Steffensen's method.

1. Introduction

This paper is aimed at studying the stationary self-consistent problem of magnetic insulation under space-charge limitation via the asymptotics of the Vlasov-Maxwell system. This approach has been introduced by Langmuir and Compton [17] and recently developed by Degond and Raviart [10], N. Ben Abdallah, P. Degond and F. M'ehats [3] to analyze the space charge limited operation of a vacuum diode. In a dimensionless form of the Vlasov-Poisson system, the ratio of the typical particle velocity at the cathode to that reached at

1991 *Mathematics Subject Classification.* 34B16, 34B18, 65L10, 82D37, 65L07, 65L08, 65L10, 65P30, 65D05, 65D10.

Key words and phrases. Magnetic insulation, singular boundary value problem, upper and lower solution, derivative free self convergent method, stiff differential equation, bifurcation.

[*] This work is supported by INTAS No. 2000-15 and grant of the National University of Colombia

[1] Departamento de Matemáticas, Facultad de Ciencias, Universidad Nacional de Colombia, Bogotá, Colombia (edulov@yahoo.com, edulov@matematicas.unal.edu.co)

[2] MIP, Laboratoire CNRS (UMR 5640), Université Paul Sabatier, 118, route de Narbonne, 31062 Toulouse Cedex, France (degond@mip.ups-tlse.fr)

[3] Departamento de Matemáticas, Facultad de Ciencias, Universidad Nacional de Colombia, Bogotá, Colombia (avsinityn@yahoo.com); MIP, Laboratoire CNRS (UMR 5640), Université Paul Sabatier, 118, route de Narbonne, 31062 Toulouse Cedex, France

the anode appears as a small parameter [10]. The associated perturbation analysis provides a mathematical framework to the results of Langmuir and Compton [17], stating that the current flowing through the diode cannot exceed a certain value called the Child-Langmuir current. This paper is concerned with an extension of this approach, based on the Child-Langmuir asymptotics to magnetized flows [3]. In particular, the value of the space charge limited current is determined when the magnetic field is small (noninsulated diode). Since the arising model could not be solved analytically, it is very important to discover its properties in noninsulated and nearly-insulated cases first.

For better understanding of the discussed mathematical problem and especially the correspondence of the numerical modelling results with a rising physical effects in vacuum diode first we need to introduce the description, how it really works.

The other related important thing is a brief discussion of the physical processes giving rise to the diode current fluctuations. The better understanding of this properties will be extremely needed for understanding current instabilities in the nearly-magnetic insulated diode. This issues will be discussed in the end of section 4.

The excellent description of this processes found in [16] is brought here.

1.1. Description of vacuum diode. The vacuum diode consists of a hot cathode surrounded by a metal anode inside an evacuated enclosure. At sufficiently high temperatures electrons are emitted from the cathode and are attracted to the positive anode. Electrons moving from the cathode to the anode constitute a current; they do so when the anode is positive with respect to the cathode. When the anode is negative with respect to the cathode, electrons are repelled by the anode and the reverse current is almost zero (due to the tail of the Maxwellian distribution of the electrons it is greater than zero). The space between the anode and the cathode is evacuated, so that electrons may move between the electrodes unimpeded by collisions with gas molecules. If $V_f = 0$ and no emission takes place, the diode may be regarded as a parallel-plate capacitor whose potential difference is V_p . In this case, the potential distribution in the cathode-plate space is represented by a straight line which joins the points corresponding to cathode potential $V_k = 0$ and the plate potential V_p . When the filament voltage rises, the electrons leaving the cathode gang up in the interelectrode space as a cloud called a space charge. This charge alters the potential distribution. Since the electrons making up the space charge are negative, the potential in the cathode-plate space goes up, though all points remain at positive potential. The vector of the electric field is directed from the plate to the cathode, so all the electrons escaping from the cathode make for the plate. In this case, the plate current equals the emission current. One could say the all electrons are being sucked away from the cathode by the anode. This region is known as the emission-limited region. As the filament voltage is increased, emission increases, and so does the space charge. Electrons having low initial velocities are driven back to the cathode by the negative space charge due to the electrons. The density of the electron cloud near the cathode increases to the point where it forms a negative potential region whose minimum, V_{\min} , is usually within a few hundredth or tenths of a millimetre of the cathode surface. Thus, there is a high retarding electric field near the cathode ($0 < x < x_{\min}$); the vector is directed away from the cathode to the plate. To overcome this field, an initial velocity v_0 of the electrons leaving the cathode

should exceed a certain value determined by V_{\min}

$$v_0 > \sqrt{2\frac{e}{m}V_{\min}}.$$

If the electron is below this value, the electron will not be able to overcome the potential barrier. It will slow down to a stop, and the field will push it back to the cathode. Accordingly, the retarding field region (from 0 to x_{\min}) contains not only electrons traveling away from the cathode, but also those falling back towards the cathode. At a constant filament voltage, a dynamic equilibrium sets in, so that the number of electrons reaching the plate and the number falling back to the cathode is equal to the number of electrons emitted by the cathode. Therefore, plate current is smaller than emission current, or the cathode produces more electrons than the anode can.

1.2. Shot noise in a diode. We know that the minimum signal observable in an electronic circuit is set by the level of electrical noise in the system. This is caused by a random fluctuation of voltage and current or electromagnetic fields. Shot noise in a diode is the random fluctuation in a diode current, I , due to the discrete nature of electronic charge. Noise causes the signal to fluctuate around a given value. The average of these fluctuations are zero, due to their randomness. But the root mean square of the fluctuation is measurable.

Perhaps a discussion of the various types of electrical noise giving rise to degradation of the observed signal, would be in order. Electrical noise may persist even after the input signal has been removed from the electronic circuit. This implies the existence of a basic limit below which signals are no longer distinguishable. The signal-to-noise ratio quantifies the observability of an output signal. Hence a measure whether satisfactory amplification can be obtained is given by this ratio. Therefore in order to ensure the maximum observability of an amplified weak signal we must ensure that the noise power introduced by the circuit devices and components should be as small as possible. External sources of noise can produce electrical interference in circuits. This may be done by electromagnetic radiation. Examples of this would be narrow-frequency band sources such as radio transmitters, local oscillators and power-supply cables and also broad-band sources such as lightning and fluorescent lamps. Another means by which electrical noise may be induced in an electronic circuit from an external source is electromagnetic induction. Since magnetic fields arise from alternating currents, thus by electromagnetic induction corresponding noise signals may be induced into other circuits or different parts of the same electronic system. In order to reduce such effects we take care in the positioning of critical circuit components to take advantage of the short range of such magnetic fields. Such effects can be greatly reduced by electrostatic screening (i.e. placing the entire circuit, or at least the sensitive portions of it, inside a closed metal box and connecting the box to earth potential). It is important that the total electrostatic screening for a system is earthed at one point only - this ensures that no large-area circuit earth-loops can exist in which signal may again be induced by electromagnetic induction. The main types of internal sources of noise present in electronic devices are thermal noise and shot noise. Thermal noise is due to the random motion of the current carriers in a metal or semiconductor which increases with temperature. Thermal noise arises from the random motion of electrons in materials due to their thermal energy of $3kT/2$ and therefore occurs even in the absence of an applied electric field.

Shot noise is due to the random flow of electrons in an electric current and is due to the particle nature of electric charge. The current flow in a vacuum diode is due to emission of electrons from the cathode which then travel to the anode. Each electron carries a discrete amount of charge and produces a small current pulse. The average anode current, I_a , is the summation of all the current pulses. The emission of electrons is a random process depending on the surface condition of the cathode, shape of electrodes, and potential between the electrodes. This gives rise to random fluctuations in the number of electrons emitted and so the diode current contains a time-varying component. Since each electron arriving at the anode is like a 'shot', the fluctuating current gives rise to a mean-square shot noise current i_s^2 .

1.3. Description of the mathematical model. We consider a plane diode consisting of two perfectly conducting electrodes, a cathode ($X = 0$) and an anode ($X = L$) supposed to be infinite planes, parallel to $(Y; Z)$. The electrons, with charge $-e$ and mass m , are emitted at the cathode and submitted to an applied electromagnetic field $\mathbf{E}_{\text{ext}} = E_{\text{ext}}X$; $\mathbf{B}_{\text{ext}} = B_{\text{ext}}Z$ such that $E_{\text{ext}} \leq 0$ and $B_{\text{ext}} \geq 0$. Such an electromagnetic field does not act on the P_Z component of the particle momentum. Hence, we shall consider a situation where this component vanishes, leading to a confinement of electrons to the plane $Z = 0$. The relationship between momentum and velocity is then given by the relativistic relations

$$\begin{cases} \mathbf{V}(\mathbf{P}) = \frac{\mathbf{P}}{\gamma m}, & \gamma = \sqrt{1 + \frac{|\mathbf{P}|^2}{m^2 c^2}} \\ \mathbf{V} = (V_X, V_Y), \mathbf{P} = (P_X, P_Y), & |\mathbf{P}|^2 = P_X^2 + P_Y^2, \end{cases} \quad (1.1)$$

which can also be written

$$\mathbf{V}(\mathbf{P}) = \nabla_{\mathbf{P}} \mathcal{E}(\mathbf{P}), \quad (1.2)$$

where \mathcal{E} is the relativistic kinetic energy

$$\mathcal{E}(\mathbf{P}) = mc^2(\gamma - 1), \quad (1.3)$$

and c is the speed of light. We shall moreover assume that the electron distribution function F does not depend on Y and that the flow is stationary and collisionless. The injection profile $G(P_X, P_Y)$ at the cathode is assumed to be given whereas no electron is injected at the anode. The system is then described by the so called 1.5 dimensional Vlasov-Maxwell model

$$V_X \frac{\partial F}{\partial X} + e \left(\frac{d\Phi}{dX} - V_Y \frac{\partial F}{\partial P_X} \right) + eV_X \frac{dA}{dX} \frac{\partial F}{\partial P_Y} = 0 \quad (1.4)$$

$$\frac{d^2 \Phi}{dX^2} = \frac{e}{\varepsilon_0} N(X), \quad X \in (0, L), \quad (1.5)$$

$$\frac{d^2 A}{dX^2} = -\mu_0 J_Y(X), \quad X \in (0, L), \quad (1.6)$$

subject to the following boundary conditions :

$$F(0, P_X, P_Y) = G(P_X, P_Y), \quad P_X > 0, \quad (1.7)$$

$$F(L, P_X, P_Y) = 0, \quad P_X < 0, \quad (1.8)$$

$$\Phi(0) = 0, \quad \Phi(L) = \Phi_L = -LE_{\text{ext}}, \quad (1.9)$$

$$A(0) = 0, \quad A(L) = A_L = LB_{\text{ext}}, \quad (1.10)$$

In this system, the macroscopic quantities, namely the particle density N , X and Y are the components of the current density J_X , J_Y . In the above equations, ε_0 and μ_0 are respectively the vacuum permittivity and permeability.

The boundary conditions are justified by the fact that the electric field $E = -d\Phi/dX$ and the magnetic field $B = -dA/dX$ are exactly equal to the external fields when self-consistent effects are ignored ($N = J_Y = 0$).

The 1.5 dimensional model (1.4)–(1.10) ignores the self-consistent magnetic field due to J_X , which would introduce two-dimensional effects, and is only an approximation of the complete stationary Vlasov-Maxwell system. In this paper we especially interested in the case, when the applied magnetic field is not strong enough to insulate the diode, J_X does not vanish and our model can be viewed as an approximation of the Maxwell equations.

In order to get a better insight in the behaviour of the diode, we write the model in dimensionless variables in the spirit of [10, 11]. We first introduce the following units respectively for position, velocity, momentum, electrostatic potential, vector potential, particle density, current and distribution function:

$$\begin{aligned} \bar{X} &= L, \quad \bar{V} = c, \quad \bar{P} = mc, \quad \mathcal{E} = mc^2, \\ \bar{\Phi} &= \frac{mc^2}{e}, \quad \bar{A} = \frac{mc}{e}, \quad \bar{N} = \frac{\varepsilon_0 \bar{\Phi}}{x \bar{X}^2}, \quad \bar{J} = -ec\bar{N}, \quad \bar{F} = \frac{\bar{N}}{\bar{P}^2}, \end{aligned}$$

and the corresponding dimensionless variables

$$\begin{aligned} x &= \frac{X}{\bar{X}}, \quad \mathbf{p} = \frac{\mathbf{P}}{\bar{P}} = (p_x, p_y), \\ \mathbf{v} = (v_x, v_y) &= \frac{\mathbf{V}}{\bar{V}} = \frac{\mathbf{p}}{\sqrt{1 + \mathbf{p}^2}}, \quad \epsilon = \frac{\mathcal{E}}{\bar{\mathcal{E}}} = \sqrt{1 + \mathbf{p}^2} - 1, \\ \varphi &= \frac{\Phi}{\bar{\Phi}}, \quad a = \frac{A}{\bar{A}}, \quad n = \frac{N}{\bar{N}}, \quad \mathbf{j} = \frac{\mathbf{J}}{\bar{J}}, \quad f = \frac{F}{\bar{F}}. \end{aligned}$$

The next step is to express that particle emission at the cathode occurs in the Child-Langmuir regime: in such a situation, the thermal velocity V_G is much smaller than the typical drift velocity supposed to be of the order of the speed of light c . Letting $\varepsilon = \frac{V_G}{c}$, we shall assume that

$$f(0, p_x, p_y) = g^\varepsilon(p_x, p_y) = \frac{1}{\varepsilon^3} g\left(\frac{p_x}{\varepsilon}, \frac{p_y}{\varepsilon}\right), \quad p_x > 0$$

where g is a given profile. The scaling factor ε^3 insures that the incoming current remains finite independently of ε , whereas the dependence on $\frac{p}{\varepsilon}$ expresses the fact that electrons are emitted at the cathode with a very small velocity. We refer to [10, 11] for a detailed discussion of the scaling. The dimensionless system reads

$$v_x \frac{\partial f^\varepsilon}{\partial x} + \left(\frac{d\varphi^\varepsilon}{dx} - v_y \frac{da^\varepsilon}{dx} \right) \frac{\partial f^\varepsilon}{\partial p_x} + v_x \frac{da^\varepsilon}{dx} \frac{\partial f^\varepsilon}{\partial p_y} = 0, \quad (1.11)$$

$$(x, p_x, p_y) \in (0, 1) \times \mathbb{R}^2,$$

$$\frac{d^2 \varphi^\varepsilon}{dx^2} = n^\varepsilon(x), \quad x \in (0, 1) \quad (1.12)$$

$$\frac{d^2 a^\varepsilon}{dx^2} = j_y^\varepsilon(x), \quad x \in (0, 1) \quad (1.13)$$

Here $n^\varepsilon(x)$ is a particle density, $j_y^\varepsilon(x)$ is a current density in Y direction. The initial and boundary conditions are also transformed

$$f^\varepsilon(0, p_x, p_y) = g^\varepsilon(p_x, p_y) = \frac{1}{\varepsilon^3} g\left(\frac{p_x}{\varepsilon}, \frac{p_y}{\varepsilon}\right), p_x > 0, \quad (1.14)$$

$$f^\varepsilon(1, p_x, p_y) = 0, p_x < 0, \quad (1.15)$$

$$\varphi^\varepsilon(0) = 0, \quad \varphi^\varepsilon(1) = \varphi_L, \quad (1.16)$$

$$a^\varepsilon(0) = 0, \quad a^\varepsilon(1) = \varphi_L, \quad (1.17)$$

Omitting the complete derivation of the limit system, when $\varepsilon \rightarrow 0$, we need to introduce some notions and notations used ahead.

DEFINITION 1.1. We define

$$\theta(x) = (1 + \varphi(x))^2 - 1 - a^2(x)$$

as an *effective potential*.

It is readily seen that electrons do not enter the diode unless the effective potential θ is nonnegative in the vicinity of the cathode. Therefore, we always have $\theta'(0) \geq 0$. The limiting case $\theta'(0) = 0$ is the space charge limited or the Child-Langmuir regime. In view (1.16), (1.16) (which still hold in the limit $\varepsilon \rightarrow 0$), this condition is equivalent to the standard Child-Langmuir condition

$$\frac{d\varphi}{dx}(0) = 0.$$

Let θ_L be the value of θ at the anode

$$\theta_L = (1 + \varphi_L)^2 - 1 - a_L^2.$$

If $\theta_L < 0$, electrons cannot reach the anode $x = 1$, they are reflected by the magnetic forces back to the cathode and the diode is said to be magnetically insulated. This enables us to define the Hull cut-off magnetic field, which is the relativistic version of the critical field introduced in [15] in the nonrelativistic case:

$$a_L^H = \sqrt{\varphi_L^2 + 2\varphi_L}.$$

The diode is magnetically insulated if $a_L > a_L^H$, and is not insulated if $a_L < a_L^H$. In dimensional variables, the Hull cut-off magnetic field is given by

$$B^H = \frac{1}{Lc} \sqrt{\Phi_L^2 + \frac{2mc^2}{e} \Phi_L}.$$

Thus our primary goal is a study of noninsulated, or nearly insulated diodes, which means $B_{\text{ext}} < B^H$. The complete derivation of the model is given in [3], while we need only its formal expressions

$$\frac{d^2\varphi}{dx^2}(x) = j_x \frac{1 + \varphi(x)}{\sqrt{(1 + \varphi(x))^2 - 1 - a^2(x)}}, \quad (1.18)$$

$$\frac{d^2a}{dx^2}(x) = j_x \frac{a(x)}{\sqrt{(1 + \varphi(x))^2 - 1 - a^2(x)}}, \quad (1.19)$$

with a corresponding Cauchy and boundary conditions

$$\varphi(0) = 0, \quad \varphi(1) = \varphi_L \quad (1.20)$$

$$\frac{d\varphi}{dx}(0) = 0 \quad (1.21)$$

$$a(0) = 0, \quad a(1) = a_L \quad (1.22)$$

Let us recall that the unknowns are the electrostatic potential φ , the magnetic potential a and the current j_x (which does not depend on x).

It is to be noticed that the whole construction of this model depends heavily on the assumption that the effective potential is positive. Actually, θ could vanish at some points in the diode, leading to closed trajectories and trapped particles.

Apart of heuristic discussions there also could be made some analytical remarks about the parametric dependences j_x, β . In particular, they are

$$(1 + \varphi(x))a'(x) - \varphi'(x)a(x) = \beta \quad (1.23)$$

$$2j_x\sqrt{\theta(x)} - (\varphi'(x))^2 + (a'(x))^2 = \beta^2 \quad (1.24)$$

The analysis of this equations were made in [3] but the proposed approach do not provide any information to be immediately used in numerical computations. Nevertheless this relations could be treated as an auxiliary method for verification of any j_x, β made.

Vector (j_x, β) hereinafter is usually refered as a parameter vector, depending on the boundary condition of the problem (1.18),(1.19). Since the analysis of the couple arbitrary chosen boundary conditions φ_L, a_L is not very usefull, we refer to $\sqrt{\theta(x)}$ and $\sqrt{\theta_L}$ especially as a distance measure. The quantities (φ_L, a_L) or $(\varphi_L, \sqrt{\theta_L})$ are algebraic equivalent on \mathbb{R}^+ to define the boundary conditions, thus we evaluate a sets of equally-distant point and refer to them as $(z, \sqrt{\theta_L})$, $z \equiv \varphi_L$.

Keeping in mind the above remarks we devote the Section 2 to the analysis of the solution trayectories, their relation with the lower and upper estimations obtained by A.V. Sinitsyn and better solution approximations. In Section two we remind some known and describe a newly developed numerical methods for solving the posed limit problem. Also there are discussed some issues of the numerical method stability in application to our problem. In the following section 4 we introduce the results of numerical experiments ,describing the properties of the parameter vector for diffrent "distances" θ_L . The numerical experiments shown that the character of the parameter curves highly depends on the quantity θ_L , being unique for $\theta_L \geq 1$ and bifurcating for $\theta_L < 1$. The accurate numerical modelling gave us a number of different parameter vectors that comply with the unique given boundary condition $(\varphi_L, \sqrt{\theta_L})$. Due to a high computation times and numerical sensivity of the problem it is difficult to evaluate the bifurcating solutions for $\theta \approx 1$ and we fixed our attention on nearly-insulated diode behaviour for $\theta_L \ll 1$. The final Section 5 describes in short the obtained results. Finally we outline the plan of the further research activities.

2. Solution trayjectory, upper and lower solutions

Finally, the limit model of magnetically noninsulation diode is described by the system of two second order ordinary differential equations (1.18),(1.19) with conditions (1.20)–(1.22).

2.1. Existence of semitrivial solutions of problem. Let us introduce the definition of cone in a Banach space X .

DEFINITION 2.1. Let X be a Banach space. A nonempty convex closed set $P \subset X$ is called a *cone*, if it satisfies the conditions:

- (i) $x \in P$, $\lambda \geq 0$ implies $\lambda x \in P$;
- (ii) $x \in P$, $-x \in P$ implies $x = \mathcal{O}$, where \mathcal{O} denotes zero element of X .

Here \leq is the order in X induced by P , i.e., $x \leq y$ if and only if $y - x$ is an element of P .

We will also assume that the cone P is normal in X , i.e., order intervals are norm bounded. In X

$$X \equiv \{(u, v) : u, v \in C^1(\bar{\Omega}), u = v = 0\}$$

we introduce the norm $|U|_X = |u|_{C^1} + |v|_{C^1}$, and the norm $|U|_X = |u|_\infty + |v|_\infty$ in C , where $U = (u, v)$. Here a cone P is given by

$$P = \{(u, v) \in X : u \geq 0, v \geq 0 \text{ for all } x \in \Omega\}.$$

So, if $u \neq 0$, $v \neq 0$ belong to P , then $-u, -v$ does not belong. We will work with classical spaces on the intervals $\bar{I} = [a, b]$, $\hat{I} =]a, b]$, $I = (a, b)$:

$C(\bar{I})$ with norm $\|u\|_\infty = \max\{|u(x)| : x \in \bar{I}\}$;

$C^1(\bar{I}) = \|u\|_\infty + \|u'\|_\infty$;

$C_{loc}(I)$, which contains all functions that are locally absolutely continuous in I . We introduce a space $C_{loc}(I)$ because the limit problem is singular for $\varphi = 0$. The order \leq in cone P is understood in the weak sense, i.e., y is increasing if $a \leq b$ implies $y(a) \leq y(b)$ and y is decreasing if $a \leq b$ implies $y(a) \geq y(b)$.

THEOREM 2.1 ((comparison principle in cone)). *Let $y \in C(\bar{I}) \cap C_{loc}(I)$. The function f is defined on $I \times R$. Let $f(x, y)$ is increasing in y function, then*

$$\begin{aligned} v'' - f(x, v) &\geq w'' - f(x, w) \text{ in mean on } I, \\ v(a) &\leq w(a), \quad v(b) \leq w(b) \end{aligned} \tag{2.1}$$

implies

$$v \leq w \text{ on } \bar{I}.$$

For the convenience of defining an ordering relation in cone P , we make a transformation for the problem (1.18)–(1.22). Let $F(\varphi, a)$ and $G(\varphi, a)$ be defined by (1.18)–(1.22). Then through the transformation $\varphi = -u$ the limit problem is reduced to the form

$$\begin{aligned} -\frac{d^2 u}{dx^2} &= j_x \frac{1-u}{\sqrt{(1-u)^2 - 1-a^2}} \triangleq \tilde{F}(j_x, u, a), \quad u(0) = 0, \quad u(1) = \varphi_L, \\ \frac{d^2 a}{dx^2} &= j_x \frac{a}{\sqrt{(1-u)^2 - 1-a^2}} \triangleq \tilde{G}(j_x, u, a), \quad a(0) = 0, \quad a(1) = a_L. \end{aligned} \tag{2.2}$$

We note that all solutions of the initial problem, as well the problem (2.2), are symmetric with respect to the transformation of sign for the magnetic potential $a : (\varphi, a) = (\varphi, -a)$ or the same $(u, a) = (u, -a)$. Thus we must search only positive solutions $\varphi > 0$, $a > 0$ in cone P or only negative ones: $\varphi < 0$, $a < 0$. Thanks to the symmetry of problem it is equivalently and does not yields the extension of the types of sign-defined solutions of the problem (1.18)–(1.22) (respect. (2.2)). Once more, we note that introduction of negative

electrostatic potential in problem (2.2) is connected with more convenient relation between order in cone and positiveness of Green function for operator $-u''$ that we use below.

DEFINITION 2.2. A pair $[(\varphi_0, a_0), (\varphi^0, a^0)]$ is called

- a) sub-super solution of the problem (1.18)–(1.22) relative to P , if the following conditions are satisfied

$$\begin{cases} (\varphi_0, a_0) \in C_{loc}(I) \cap C(\bar{I}) \times C_{loc}(I) \cap C(\bar{I}), \\ (\varphi^0, a^0) \in C_{loc}(I) \cap C(\bar{I}) \times C_{loc}(I) \cap C(\bar{I}) \end{cases} \quad (2.3)$$

$$\varphi_0'' - j_x \frac{1 + \varphi_0}{\sqrt{(1 + \varphi_0)^2 - 1 - a^2}} \triangleq F(\varphi_0, a) \leq 0 \text{ in } I,$$

$$(\varphi^0)'' - j_x \frac{1 + \varphi^0}{\sqrt{(1 + \varphi^0)^2 - 1 - a^2}} \triangleq F(\varphi^0, a) \geq 0 \text{ in } I \quad \forall a \in [a_0, a^0];$$

$$a_0'' - j_x \frac{a_0}{\sqrt{(1 + \varphi)^2 - 1 - a_0^2}} \triangleq G(\varphi, a_0) \leq 0 \text{ in } I,$$

$$(a^0)'' - j_x \frac{a^0}{\sqrt{(1 + \varphi)^2 - 1 - (a^0)^2}} \triangleq G(\varphi, a^0) \geq 0 \text{ in } I \quad \forall \varphi \in [\varphi_0, \varphi^0];$$

$$\varphi_0 \leq \varphi^0, \quad a_0 \leq a^0 \text{ in } I$$

and on the boundary

$$\begin{aligned} \varphi_0(0) \leq 0 \leq \varphi^0(0), \quad \varphi_0(1) \leq \varphi_L \leq \varphi^0(1), \\ a_0(0) \leq 0 \leq a^0(0), \quad a_0(1) \leq a_L \leq a^0(1); \end{aligned}$$

- b) sub-sub solution of the problem (1.18)–(1.22) relative to P , if a condition (3.4) is satisfied and

$$\begin{aligned} \varphi_0'' - F(j_x, \varphi_0, a_0) \leq 0 \text{ in } I, \\ a_0'' - G(j_x, \varphi_0, a_0) \leq 0 \text{ in } I \end{aligned} \quad (2.4)$$

and on the boundary

$$\varphi_0(0) \leq 0, \quad \varphi_0(1) \leq \varphi_L, \quad a_0(0) \leq 0, \quad a_0(1) \leq a_L. \quad (2.5)$$

REMARK 2.1. In Definition 2.2 the expressions with square roots we take by modulus $|(1 + \varphi)^2 - 1 - a^2|$.

By analogy with (2.4), (2.5), we may introduce the definition of super-super solution in cone.

DEFINITION 2.3. The functions $\Phi(x, x_{a_i}, j_x)$, $\Phi_1(x, x_{\varphi_j}, j_x)$ we shall call a *semitrivial solutions* of the problem (1.18)–(1.22), if $\Phi(x, x_{a_i}, j_x)$ is a solution of the scalar boundary value problem

$$\begin{aligned} \varphi'' = F(j_x, \varphi, x_{a_i}) = j_x \frac{1 + \varphi}{\sqrt{(1 + \varphi)^2 - 1 - (x_{a_i})^2}}, \\ \varphi(0) = 0, \quad \varphi(1) = \varphi_L, \end{aligned} \quad (2.6)$$

and $\Phi_1(x, x_{\varphi_j}, j_x)$ is a solution of the scalar boundary value problem

$$a'' = G(j_x, x_{\varphi_j}, a) = j_x \frac{a}{\sqrt{(1 + x_{\varphi_j})^2 - 1 - a^2}}, \quad (2.7)$$

$$a(0) = 0, \quad a(1) = a_L.$$

Here x_{a_i} , $i = 1, 2, 3$ and x_{φ_j} , $j = 1, 2$ are respectively, the *indicators* of semitrivial solutions $\Phi(x, x_{a_i}, j_x)$, $\Phi_1(x, x_{\varphi_j}, j_x)$ defined by the following way:

$$x_{a_1} = 0, \text{ if } a(x) = 0;$$

$$x_{a_2} = a^0, \text{ if } a = a^0 \text{ be upper solution of the problem (2.7);}$$

$$x_{a_3} = a_0, \text{ if } a = a_0 \text{ be lower solution of the problem (2.7);}$$

$$x_{\varphi_1} = \varphi^0, \text{ if } \varphi = \varphi^0 \text{ be upper solution of the problem (2.6);}$$

$$x_{\varphi_2} = \varphi_0, \text{ if } \varphi = \varphi_0 \text{ be lower solution of the problem (2.6).}$$

From Definition 2.3, we obtain the following types of scalar boundary value problems for semitrivial (in sense of Definition 2.3) solutions are

$$\varphi'' = F(\varphi, 0) = j_x \frac{1 + \varphi}{\sqrt{(1 + \varphi)^2 - 1}}, \quad \varphi(0) = 0, \quad \varphi(1) = \varphi_L. \quad (A_1)$$

$$\varphi'' = F(\varphi, a^0) = j_x \frac{1 + \varphi}{\sqrt{(1 + \varphi)^2 - 1 - (a^0)^2}}, \quad \varphi(0) = 0, \quad \varphi(1) = \varphi_L. \quad (A_2)$$

$$\varphi'' = F(\varphi, a_0) = j_x \frac{1 + \varphi}{\sqrt{(1 + \varphi)^2 - 1 - (a_0)^2}}, \quad \varphi(0) = 0, \quad \varphi(1) = \varphi_L. \quad (A_3)$$

$$a'' = G(\varphi^0, a) = j_x \frac{a}{\sqrt{(1 + \varphi^0)^2 - 1 - a^2}}, \quad a(0) = 0, \quad a(1) = a_L. \quad (A_4)$$

$$a'' = G(\varphi_0, a) = j_x \frac{a}{\sqrt{(1 + \varphi_0)^2 - 1 - a^2}}, \quad a(0) = 0, \quad a(1) = a_L. \quad (A_5)$$

We shall find the solutions of problems (A₁) – (A₃) for $\varphi_0 < \varphi^0$, where $\varphi_0(x_{a_1})$, $\varphi^0(x_{a_2})$ are respectively, lower and upper solutions of problem (A₁). The solution (φ, a) of the initial problem should be belong to the interval

$$\varphi \in \Phi(\varphi, 0) \cap \Phi(\varphi, a^0) \cap \Phi(\varphi, a_0),$$

$$a \in \Phi_1(\varphi^0, a) \cap \Phi_1(\varphi_0, a).$$

Moreover, the ordering of lower and upper solutions of problems (A₁) – (A₃) is satisfied

$$\varphi_0(x_{a_1}) < \varphi_0(x_{a_2}) < \varphi_0(x_{a_3}) < \varphi^0(x_{a_2}) < \varphi^0(x_{a_1}).$$

We shall seek the solution of problems (A₄) – (A₅) for $a_0 < a^0$. In this case the following ordering of lower and upper solutions of problems (A₄) – (A₅)

$$a_0(x_{\varphi_1}) < a_0(x_{\varphi_2}) < a^0(x_{\varphi_2}) < a^0(x_{\varphi_1}).$$

is satisfied.

We go over to the direct study of the problem (2.6) which includes the cases (A₁) – (A₃). Let us consider the boundary value problem (2.6) with

$$F(x, \varphi) : (0, 1] \times (0, \infty) \rightarrow (0, \infty). \quad (B_1)$$

In condition (B_1) for $F(x, \varphi)$ we dropped index a_i , considering a general case of nonlinear dependence F of x .

We shall assume that F is a Caratheodory function, i.e.,

$$F(\cdot, s) \text{ measurable for all } s \in R, \quad (B_2)$$

$$F(x, \cdot) \text{ is continuous a.e. for } x \in]0, 1], \quad (B_3)$$

and the following conditions hold

$$\int_0^1 s(1-s)F ds < \infty. \quad (B_4)$$

$$\partial F / \partial \varphi > 0, \text{ i.e., } F \text{ is increasing in } \varphi. \quad (B_5)$$

There are $\gamma(x) \in L^1(]0, 1])$ and $\alpha \in R, 0 < \alpha < 1$ such that

$$|F(x, s)| \leq \gamma(x)(1 + |s|^{-\alpha}), \quad \forall (x, s) \in]0, 1] \times R. \quad (B_6)$$

We are interested in a positive classical solution of equation (2.6), i.e., $\varphi > 0$ in P for $x \in]0, 1]$ and $\varphi \in C([0, 1]) \cap C^2(]0, 1])$. The problem (2.6) is singular, therefore, condition (B_1) is not fulfilled on the interval $\varphi \in (0, \infty)$ and in this connection, the well-known theorems on existence of lower and upper solution in cone P does not work. It follows from Theorem 2.1, since F in (2.6) is increasing in φ , then $\varphi < w$ for $x \in]0, 1]$, where φ and w satisfy the differential inequality (2.1).

THEOREM 2.2. *Assume conditions $(B_2) - (B_6)$. Then there exists a positive solution $\varphi \in C([0, 1]) \cap C^2(]0, 1])$ of the boundary value problem (2.6).*

Application of monotone iteration techniques to the equation (2.6) gives an existence of maximal solution $\bar{\varphi}(x, j_x)$ such that

$$\varphi(x, x_j) \leq \bar{\varphi}(x, x_j) < w(x) \text{ for } x \in]0, 1].$$

PROPOSITION 2.3. *Let $0 < c \leq j_x \leq j_x^{max}$. Then equation (A_1)*

$$\varphi'' = F(j_x, \varphi, 0) = j_x \frac{1 + \varphi}{\sqrt{\varphi(2 + \varphi)}},$$

$$\varphi(0) = 0, \quad \varphi(1) = \varphi_L$$

has a lower positive solution

$$u_0 = \delta^2 x^{4/3}, \quad (2.8)$$

if

$$4\delta^3 \geq 9j_x^{max}(1 + \delta^2)/\sqrt{2 + \delta^2} \quad (2.9)$$

and an upper positive solution

$$u^0 = \alpha + \beta x \quad (\alpha, \beta > 0) \quad (2.10)$$

with

$$\varphi_L \geq \delta^2, \quad (2.11)$$

where δ is defined from (2.9).

REMARK 2.2. Square root is taking as $\sqrt{|\varphi(2 + \varphi)|}$ in the case of negative solutions. Here $u^0 = -\epsilon x$ is an upper solution, and $u_0 = -2 + \epsilon$ is a lower solution ($0 < \epsilon < 1$). Hence equation (A_1) has the negative solution only for $0 < \varphi_L < -2$ because $F(x, -2) = -\infty$.

It follows from (2.9), (2.11) that a value of current is limited by the value of electrostatic potential on the anode φ_L

$$j_x \leq j_x^{max} \leq \mathcal{F}(\varphi_L). \quad (2.12)$$

Analysis of lower and upper solutions (2.8), (2.10) exhibits that for $\delta^2 = \varphi_L > 2$ and $\alpha = \beta \leq 1$ interval in x between lower and upper solutions is decreased, and for the large values of the potential φ_L diode makes on regime $\varphi_L x^{4/3}$.

PROPOSITION 2.4. *Let $0 < c \leq j_x \leq j_x^{max}$. Then equation (A_4)*

$$a'' = G(j_x, \varphi^0, a) = j_x \frac{a}{\sqrt{(1 + \varphi^0)^2 - 1 - a^2}}, \quad a(0) = 0, \quad a(1) = a_L$$

with a lower solution $a_0 = 0$ and an upper solution $a^0 = u^0 > 0$, conditions (3.14), (3.16) has an unique solution $a(x, j_x, c)$, which is positive, moreover

$$0 \leq a_L \leq \sqrt{\varphi^0(2 + \varphi^0)}.$$

REMARK 2.3. The problem (A_5) is considered by analogy with problem (A_4) , change of an upper solution $a^0 = u^0$ to a lower $a^0 = u_0$ one and $0 \leq a_L \leq \sqrt{\varphi_{0L}(2 + \varphi_{0L})}$.

Following to the definition 2.2 and Propositions 2.3, 2.4, solutions of the problems (2.6), (2.7) we can write in the form lower-lower (φ_0, a_0) :

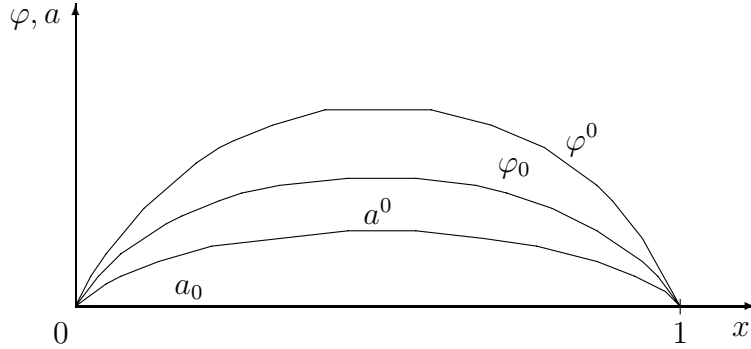


Figure 2.1: location of lower (φ_0, a_0) and upper (φ^0, a^0) solutions

$$\varphi_0 = u_0 = \delta^2 x^{4/3}, \quad a_0 = 0, \quad \varphi_L \geq \delta^2;$$

upper-lower (φ^0, a_0) :

$$\varphi^0 = u^0 = \alpha + \beta x, \quad a_0 = 0, \quad \delta^2 \leq \varphi_L \leq \mathcal{C}, \quad \mathcal{C} = \max\{\alpha, \beta\};$$

lower-upper (φ_0, a^0) :

$$\varphi_0 = u_0 = \delta^2 x^{4/3}, \quad a^0 = u^0, \quad \varphi_L \geq \delta^2, \quad a_L \leq \sqrt{(u_0(2 + u_0))};$$

upper-upper (φ^0, a^0) :

$$\varphi^0 = u^0 = \alpha + \beta x, \quad a^0 = u^0, \quad \varphi_L \leq \mathcal{C}, \quad a_L \leq a^0 \leq u^0.$$

Thus we have the following main result:

THEOREM 2.5. *Assume conditions (B_2) , (B_3) , (B_6) and inequalities (3.14), (3.17) and*

$$a_L \leq \frac{j_x}{2} \leq \frac{j_x^{max}}{2} \leq \frac{\mathcal{F}(\varphi_L)}{2}$$

fulfilled. Then the problem (1.18)–(1.22) possesses a positive solution in cone P such that

$$\begin{cases} \varphi_0'' \geq j_x F(\varphi_0, z_2), & z_2 \in [0, \varphi^0] \\ (\varphi^0)'' \leq j_x F(\varphi^0, z_2), & z_2 \in [0, \varphi^0] \end{cases},$$

$$\begin{cases} a_0'' \geq G(j_x, z_1, a_0), & z_1 \in [\varphi_0, \varphi^0] \\ (a^0)'' \leq G(j_x, z_1, a^0), & z_1 \in [\varphi_0, \varphi^0] \end{cases},$$

where $\varphi_0 = \delta^2 x^{4/3}$ is a lower solution of problem (A_1) , $\varphi^0 = \alpha + \beta x$ ($\alpha, \beta > 0$) is an upper solution of problem (A_1) with condition $\varphi_L \geq \delta^2$; $a_0 = 0$ is a lower solution of problem (A_4) with condition $0 \leq a_L \leq \sqrt{\varphi^0(2 + \varphi^0)}$.

2.2. Analysis of the known upper and lower solutions. Up to this moment the analytical solution of the ODE system defined by (1.18),(1.19) with respect to the conditions (1.20)–(1.22) is unknown. The only nown result partially describing the form of the solution trayectory was given 2.3, see also [26]. According to it, both solution trayectories are bounded by the upper and lower solutions

$$y_{UP}(x) = kx + b, \quad k, b > 0 \quad (2.13)$$

$$y_{LOW}(x) = c^2 x^{\frac{4}{3}} \quad (2.14)$$

Using the boundary conditions (1.20),(1.22) one can obtain a quite good solution trayectory estimations

$$c^2 \varphi_L x^{\frac{4}{3}} \leq \varphi(x) \leq \varphi_L x, \quad 0 \leq a(x) \leq a_L x$$

defined on $x \in [0, 1]$. Here and everywhere we assume boundary conditions φ_l , a_L correctly defined, i.e. $\theta_L > 0$. Looking forward and leaving the discussion of numerical solution methods for next the sections, here we provide some numerical solution trayectory examples both for $\varphi(x)$ and $a(x)$ evaluated for different boundary conditions.

The strightforward analysis of the trayectories fig. 2.2–2.4 shows, that the lower solutions obtained in the section 2.1 could be made significantly better and the upper solutions are exactly $\varphi_L x$ and $a_L x$. The lower solution obviously could be written as

$$y_{LOW}(x) = y(1)x^\gamma, \quad \gamma > 1. \quad (2.15)$$

Here $y(1)$ is ether φ_L or a_L . The value of the parameter γ depends only on φ_L , a_L and could be found numerically.

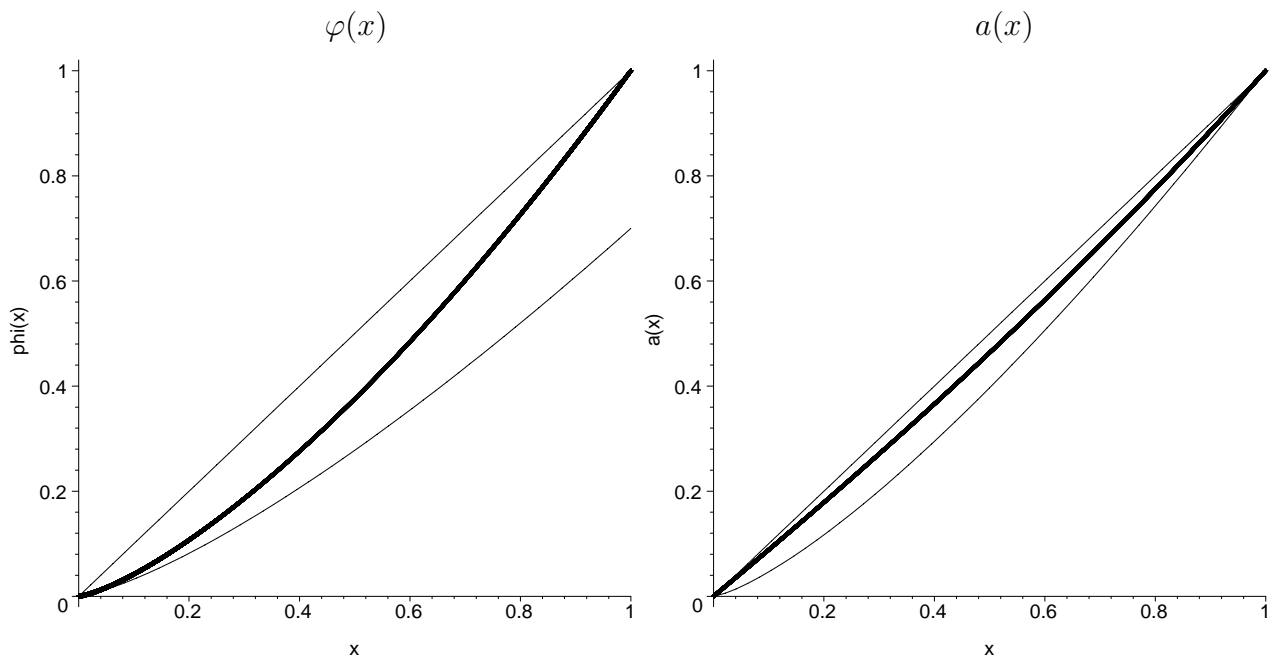


Figure 2.2: Numerical solution for $\varphi_L = a_L = 1$; numerical integration error $\varepsilon_\varphi = 2.4611389315421e - 17$, $\varepsilon_a = 6.13116328540553e - 17$; estimated $j_x = 0.534075023488271$, $\frac{da}{dx}(0) = 0.879738089874635$. Function $\varphi(x)$: upper solution $y = x$ and lower solution $y = \frac{7}{10}x^{\frac{4}{3}}$. Function $a(x)$: upper solution $y = x$ and lower solution $y = x^{\frac{4}{3}}$.

2.3. First lower solution hypothesis. First, we suggested that (2.15) could be the exact solution for $\varphi(x)$ and $a(x)$. In this case at each point of the numerical solution we should have

$$\begin{aligned}\hat{\varphi}(x_i) &= \varphi_L x_i^{\gamma_\varphi} \\ \hat{a}(x_i) &= a_L x_i^{\gamma_a}.\end{aligned}\tag{2.16}$$

Here and elsewhere we denote by $\hat{y}(x)$ a numerical solution of any ODE $y(x)$. Hence

$$\gamma_\varphi = \frac{\ln \frac{\hat{\varphi}(x_i)}{\varphi_L}}{\ln x_i}, \quad \gamma_a = \frac{\ln \frac{\hat{a}(x_i)}{a_L}}{\ln x_i}\tag{2.17}$$

and the best way to verify this hypothesis is to evaluate the mean m and dispersion σ^2 for each boundary condition pair available.

Using the same data of numerical integration with 50000 segments and rejecting the initial and boundary points we have a 49999 number sample. The results of this statistical estimation are included in the table 2.1.

As it will be explained in section 3, the problem (1.18),(1.19) is highly numerically sensitive, thus even a moderate diminishing of integration step can remarkably improve the estimations for γ . Thus we provide the same results, calculated from the 75000 segments of numerical integration. Omitting the initial and boundary integration points we have a 74999 number sample.

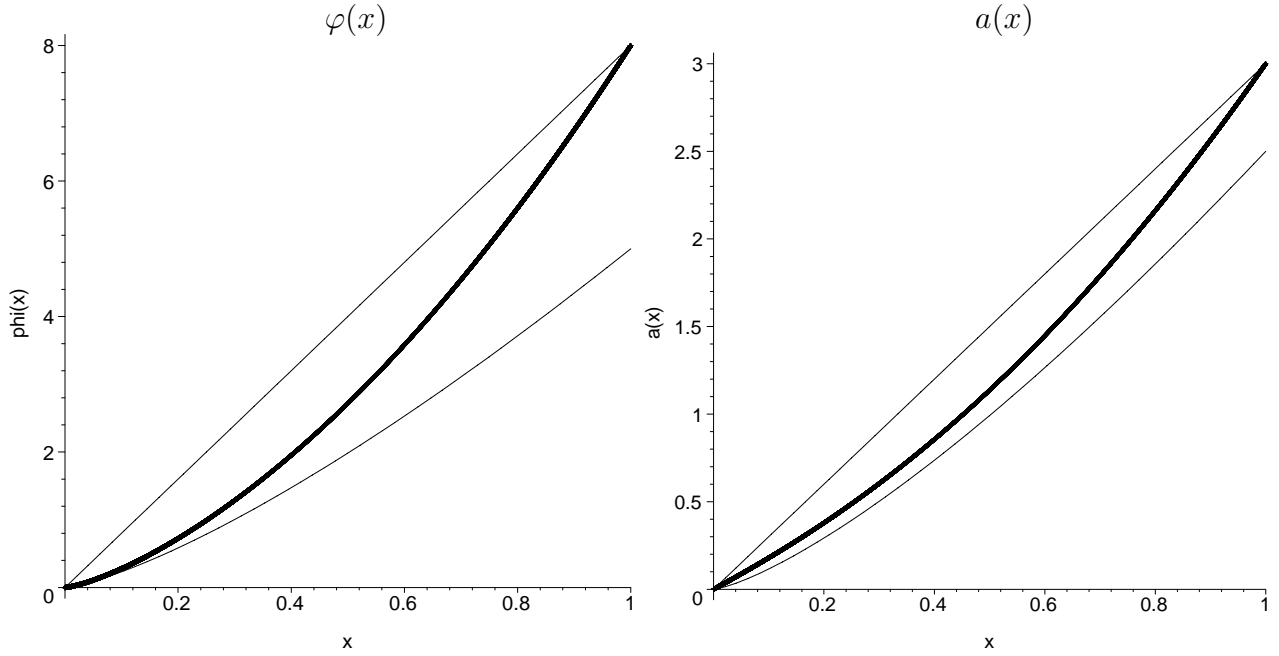


Figure 2.3: Numerical solution for $\varphi_L = 8$, $a_L = 3$; numerical integration error $\varepsilon_\varphi = 3.27429056090622e - 16$, $\varepsilon_a = 1.19262238973405e - 17$; estimated $j_x = 8.93859989164142$, $\frac{da}{dx}(0) = 1.72776197665836$. Function $\varphi(x)$: upper solution $y = 8x$ and lower solution $y = 5x^{\frac{4}{3}}$. Function $a(x)$: upper solution $y = 3x$ and lower solution $y = \frac{5}{2}x^{\frac{4}{3}}$.

Table 2.1: γ parameter estimation; 49999 sample points.

φ_L	a_L	m_{γ_φ}	$\sigma_{\gamma_\varphi}^2$	m_{γ_a}	$\sigma_{\gamma_a}^2$
1.0	1.0	1.40997395320377060253	$5.285e - 4$	1.10596987856885963230	$1.327e - 3$
8.0	3.0	1.54517548738054795197	$3.255e - 3$	1.37634131393335331450	$1.006e - 2$
0.3	0.8	1.48384932940527693565	$2.937e - 3$	1.05226600352745440305	$5.148e - 4$

Table 2.2: γ parameter estimation; 74999 sample points.

φ_L	a_L	m_{γ_φ}	$\sigma_{\gamma_\varphi}^2$	m_{γ_a}	$\sigma_{\gamma_a}^2$
1.0	1.0	1.40980550718292391143	$5.326e - 4$	1.10592470934005674719	$1.328e - 3$
8.0	3.0	1.54499486502313331624	$3.267e - 3$	1.37624420694201759187	$1.0065e - 2$
0.3	0.8	1.48367876763135441401	$2.947e - 3$	1.05223391870189564701	$5.155e - 4$

The numbers presented in the table 2.2 are nearly the same and even slightly worse, because the real numerical computational error in both cases is about 10^{-16} – 10^{-17} . That is too close to the numerical tolerance of the 80 bit floating point hardware computations.

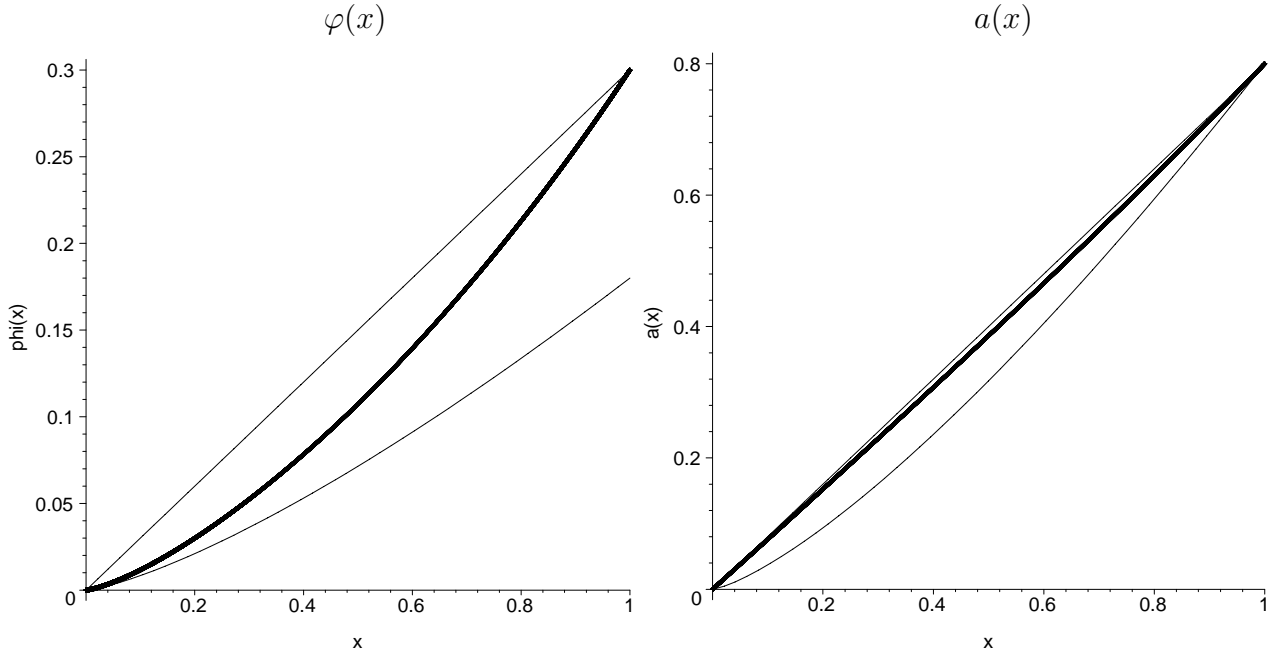


Figure 2.4: Numerical solution for $\varphi_L = 0.3$, $a_L = 0.8$; numerical integration error $\varepsilon_\varphi = 1.71574993795831e - 17$, $\varepsilon_a = 5.97937498125756e - 17$; estimated $j_x = 0.0761231763035411$, $\frac{da}{dx}(0) = 0.759092882499624$. Function $\varphi(x)$: upper solution $y = 0.3x$ and lower solution $y = 0.18x^{\frac{4}{3}}$. Function $a(x)$: upper solution $y = 0.8x$ and lower solution $y = 0.8x^{\frac{4}{3}}$.

Using hypotesis (2.15) and substituting in equations (1.18),(1.19) with respect to the conditions (1.20)–(1.22) we obtain two quadratic equations

$$\begin{aligned} \gamma_\varphi^2 - \gamma_\varphi - \frac{1 + \varphi_L}{\varphi_L} \xi_L &= 0 \\ \gamma_a^2 - \gamma_a - \xi_L &= 0 \end{aligned}$$

where $\xi_L \equiv \frac{j_x}{\sqrt{\theta_L}}$. Using the assumption $\gamma > 1$ we get

$$\gamma_\varphi = \frac{1}{2} \left(1 + \sqrt{1 + 4\xi_L + \frac{1}{\varphi_L}} \right), \quad (2.18)$$

$$\gamma_a = \frac{1}{2} \left(1 + \sqrt{1 + 4\xi_L} \right). \quad (2.19)$$

It immediately follows that $\gamma_\varphi > \gamma_a$, that comply with results in table 2.1. Substituting example data we obtain

Obviously, being substituted in (2.16), the numbers from the table 2.3 represent functions, passing below the numerical trajectory solution curve.

2.4. Second lower solution hypotesis. Comparing numbers from tables 2.1, 2.3 we see that (2.16) lower solution are passing below the real solutions trajectories. And, that is much more important, the behaviour of the lower solution for $a(x)$ do not correspond the

Table 2.3: Hypotesis (2.15) γ parameter estimation.

φ_L	a_L	γ_φ	γ_a
1.0	1.0	1.436828731	1.292242432
8.0	3.0	1.658475999	1.644909010
0.3	0.8	1.693216882	1.268396508

initial condition $\frac{da}{dx}(0) \neq 0$. Hence we can suppose that the real solution curve (or at least its estimation) should be expressed in the form like

$$\bar{a}(x) = c_1 x - c_2 x^{\gamma_a} . \quad (2.20)$$

Applying conditions (1.20)–(1.22) to the equation (2.20) we obtain the system of equations

$$\left\{ \begin{array}{l} \bar{a}(0) = 0 \\ \bar{a}(1) = c_1 + c_2 = a_L \\ \frac{d\bar{a}}{dx}(0) = c_1 \\ \frac{d^2\bar{a}}{dx^2}(1) = -c_2 \gamma_a (\gamma_a - 1) \end{array} \right.$$

Using equation (1.19) we obtain

$$\left\{ \begin{array}{l} c_1 = \frac{da}{dx}(0) \\ c_2 = \frac{da}{dx}(0) - a_L \\ \gamma_a^2 - \gamma_a + \frac{a_L}{\frac{da}{dx}(0) - a_L} \xi_L = 0 \end{array} \right. \quad (2.21)$$

Calculating the positive solution on γ_a we have

$$\bar{a}(x) = \frac{da}{dx}(0)x - \left(\frac{da}{dx}(0) - a_L \right) x^{\frac{1}{2} \left(1 + \sqrt{1 + 4\xi_L \frac{a_L}{\frac{da}{dx}(0) - a_L}} \right)} . \quad (2.22)$$

Using the same experimental data we found

Table 2.4: Hypotesis (2.20) parameter estimation.

φ_L	a_L	c_1	c_2	γ_a
1.0	1.0	0.879738089874635	-0.120261910125365	2.34125323504098515435
8.0	3.0	1.72776197665836	-1.27223802334164	2.15875192601523297264
0.3	0.8	0.759092882499624	-0.040907117500376	3.12824682869384663658

The above functions are illustrated below Taking a glance on the curves 2.5 and curves 2.2–2.4 one can see a better correspondence of the newly proposed estimation (2.22).

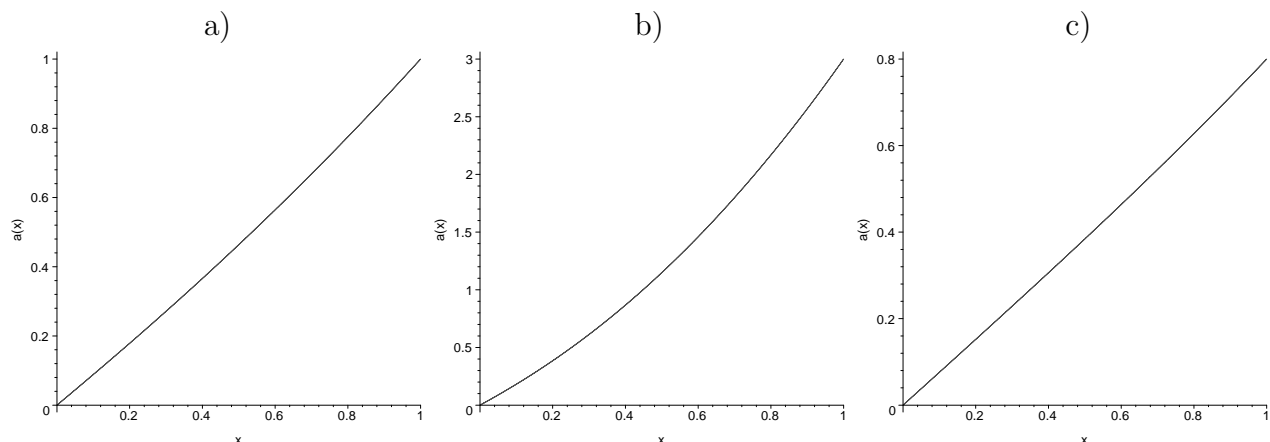


Figure 2.5: Hypotesis (2.20). a) $\varphi_L = a_L = 1.0$; b) $\varphi_L = 8.0$, $a_L = 3.0$; c) $\varphi_L = 0.3$, $a_L = 0.8$.

To verify this hypotesis by means of statistical approach we will use the same idea as above. Assuming c_1 , c_2 to be known, we evaluate the mean and dispersion for γ_a in (2.20) to compare them with analytical data, given in table 2.3. Since the relation

$$\frac{\hat{a}(x_i) - c_1 x_i}{c_2}$$

could be negative due to the computational error of numerical intergration, we will consider only the valid points of the whole samples. The table 2.5 provides a truncated estimations

Table 2.5: Hypotesis (2.15) γ_a parameter estimation.

φ_L	a_L	Valid points	γ_a	m_{γ_a}	$\sigma_{\gamma_a}^2$	ε_A	ε_N
1.0	1.0	48744	2.34125	2.36129	$2.182e - 3$	22.54118	22.50162
8.0	3.0	49438	2.15875	2.23132	$1.999e - 3$	245.63749	243.99216
0.3	0.8	47833	3.12825	2.67611	$1.126e - 2$	6.98219	7.21990

for the parameter γ_a rejecting lower significant digits without loss of statistical relevance. Comparing columns four and five we see that according to numerical estimation the function (2.20) will pass above its analytically estimated analog in the third example for $\varphi_L = 0.3$, $a_L = 0.8$ and below in the two first ones. It means that such a remarkable difference of the estimations have to be studied more attentively.

To make such an analysis, the table 2.5 contain the two last columns entitled ε_A and ε_N representing the euclidean norm of the vector difference $\hat{a}(x) - \bar{a}(x)$ evaluated for two different parameters γ_a : analytically estimated (see table 2.4) and statistically estimated (see table 2.5, all estimation digits were used in computations). In the third line we see that an analytical estimation is better then the statistical one but the mistake levels are close in all three examples.

To verify this idea we have to compare the values

$$\bar{a}'(1) = c_1 \cdot 1 - c_2 \cdot \gamma_a \cdot x^{\gamma_a - 1} = \frac{da}{dx}(0) - \left(\frac{da}{dx}(0) - a_L\right)\gamma_a$$

for all three numerical experiments:

Exp.	Hypotesis	Calculated
1	1.16130167600785401476	1.16218421557717
2	4.47420825989693827300	4.51242935767056
3	0.88706044309118177670	0.87651519455565

where the third column is the numerically calculated derivative $\hat{a}'(1)$.

Definitely this results prove our estimation defined by formula (2.22) are consistent. But, leaving the initial point with the same tangent as a numerical solution, we came to the final one with a smaller in two cases. It mean that the curve (2.22) definitely is not a lower solution, but it could be assumed as a quite good approximation of a solution $a(x)$.

3. Numerical methods

3.1. Formal analysis of limit problem. The second order ODE system (1.18),(1.19)

$$\frac{d^2\varphi}{dx^2}(x) = j_x \frac{1 + \varphi(x)}{\sqrt{(1 + \varphi(x))^2 - 1 - a^2(x)}},$$

$$\frac{d^2a}{dx^2}(x) = j_x \frac{a(x)}{\sqrt{(1 + \varphi(x))^2 - 1 - a^2(x)}},$$

is not completely defined by its initial and boundary conditions (1.20)–(1.22)

$$\begin{aligned} \varphi(0) &= 0, \quad \varphi(1) = \varphi_L \\ \frac{d\varphi}{dx}(0) &= 0 \\ a(0) &= 0, \quad a(1) = a_L \end{aligned}$$

since application of any numerical integration method for Cauchy problem (1.18),(1.19) require values

$$\begin{aligned} \varphi(0) &= 0, \quad \frac{d\varphi}{dx}(0) = 0 \\ a(0) &= 0, \quad \frac{da}{dx}(0) = \beta \end{aligned}$$

to be given. Here the last of the initial conditions is unknown, as well as a "parameter"–constant j_x . Therefore we need to define this to variables j_x, β as unknown parameters. Depending on this, pair $p = (j_x, \beta)$ we will reach the different final trayectory points $\varphi(1, j_x, \beta)$ and $a(1, j_x, \beta)$. To remove this obstacle we a invesigating the boundary problem

$$\mathfrak{F}(j_x, \beta) = \begin{pmatrix} \varphi(1, j_x, \beta) - \varphi_L \\ a(1, j_x, \beta) - a_L \end{pmatrix} = 0 \quad (3.1)$$

being defined by a nonlinear function $\mathfrak{F}(j_x, \beta)$.

And using only all the equations (1.18),(1.19), (1.20)–(1.22) and (3.1) the limit problem becomes completely defined. But the new problem immediatly arise. Namely, the analytical solution of the system (1.18),(1.19) is unknown. Then we can not apply any of the already

known methods for solving a vector system of nonlinear equations (3.1). For example, the application of the Newton method

$$x_{i+1} = x_i - \left[\frac{\partial \mathfrak{F}}{\partial p} \right]^{-1} (x_i) \mathfrak{F}(x_i)$$

require the Jacobian $J = \frac{\partial \mathfrak{F}}{\partial p}$ to be analytically known.

On the other hand, one can revise that system (1.18),(1.19) is singlar at $x \equiv 0$. A carefull study of this equations shows that considering $\varphi^{(2)}(0) \equiv a^{(2)}(0) = Const$ for arbitrary constant value makes a system (1.18),(1.19) consistent analytically. On the other hand, the only numerically accepted values are the real solution trayectory convexity numbers.

It immediately follows that all explicit numerical ODE solution methods are unapplicable in starting point. The numerical experiments also shown the equations (1.18),(1.19) are highly sensitive to the value of numerical integration step h . Here we give the table containing the \mathfrak{F} values evaluated for different $h = 1/n$ with the same $p = (j_x, \beta)$ given. For the numerical

Table 3.1: Numerical integration errors

n	ε_φ	ε_a
1000	1.61425217900765E-0002	-4.47533487147775E-0003
2500	8.34380843012195E-0003	-2.46343215088107E-0003
5000	4.68455678253690E-0003	-1.52983203144597E-0003
10000	2.27729848639435E-0003	-9.16751253617249E-0004
50000	-5.55677931763120E-0004	-1.91669763913965E-0004

integration of the system (1.18),(1.19) we used standard implicit Euler second order method

$$y_{i+1} = y_i + hf(x_{i+1}, y_{i+1})$$

along with a standard Newton's method to solve this nonlinear equation.

Comparing the rows (1, 4) and (3, 5) in the table 3.1 we see that a change of integration step size by 10 changes the global integration error by the order of 10 also, not 100 time, as it could be expected. Using any numerical analysis textbook a reader could find a lot of examples with a second order convergence speed that need even greater integration steps, about 10^{-2} .

Then the unique acceptable integration method is the Gear's methods, see [6], [13], [14].

3.2. Gear's method and problem numerical sensivity. Here we provide only a very short resume of the general results, given in [13] and in later papers.

It is well known that classical Gear's iterative methods of the M -th consistency order are written as

$$Y_{i+1}^{(k+1)} = \sum_{k=1}^M (hb_{M-k} f_{i+1-k} - a_{M-k} Y_{i+1-k}) + hb_M f_{i+1}^{(k)}. \quad (3.2)$$

Here $f_{i+1}^{(k)} = f(x_{i+1}, Y_{i+1}^{(k)})$, upper index k denote an iteration number. The idea is to make some iterative approximations starting from the fixed, already evaluated solution points. For better explanation of the formula (3.2) we put three low consistency order methods in the table 3.2.

Table 3.2: Gear's iterative method of q -th consistency order

Order q	Expression
1	$Y_{i+1}^{(k+1)} = Y_i + hf(x_{i+1}, Y_{i+1}^{(k)})$
2	$Y_{i+1}^{(k+1)} = \frac{1}{3} \left(4Y_i - Y_{i-1} + 2hf(x_{i+1}, Y_{i+1}^{(k)}) \right)$
3	$Y_{i+1}^{(k+1)} = \frac{1}{11} \left(18Y_i - 9Y_{i-1} + 2Y_{i-2} + 6hf(x_{i+1}, Y_{i+1}^{(k)}) \right)$

One can see that the 1-st consistency order method is equal to the simple-iteration implicit Euler method and it is just the matter of fact that an implicit Euler method is the simplest numerical method applicable for solution of the stiff differential equations.

Comparing the notions of the numerical method convergence order and consistency order for the implicit Euler method with respect to numbers given in the table 3.1 we see that a consistency order is kept for the problem (1.18),(1.19). It seems to be a little strange, but Gear's method for $q = 2$ proved himself as more sensitive and the computational time for a desired error level was only little better compared with $q = 1$. Hence we implemented this method in the developed software, but never used it in the main modelling.

The explanation of this fact lies in the convergence conditions of Gear iterations (3.2). Let $\|\cdot\|$ is some matrix norm, $\frac{\partial f(x, y)}{\partial y}$ – function Jacobian. Then Gear iterations converge iff

$$\left\| hb_M \frac{\partial f}{\partial y} \right\| < 1. \quad (3.3)$$

3.3. Reduced problem statement. To apply any of the mentioned numerical methods and to study their convergence properties we reduce the system of second order ODE's (1.18),(1.19) to the system of first order ODE's

$$\begin{aligned} y_1' &= y_2 \\ y_2' &= j_x \frac{1 + y_1}{\sqrt{(1 + y_1)^2 - 1 - y_3^2}} \\ y_3' &= y_4 \\ y_4' &= j_x \frac{y_3}{\sqrt{(1 + y_1)^2 - 1 - y_3^2}} \\ \bar{y}_0 &= (y_1(0), y_2(0), y_3(0), y_4(0)) = (0, 0, 0, \beta). \end{aligned} \quad (3.4)$$

System (3.4) is the autonomous ODE system and has a smaller computational cost. Moreover, if we could overcome its "stiffness", there are a number of special effective implicit numerical methods for solving this type of ODE systems.

Hence we have to estimate the Jacobian of the system (3.4) near the singular initial point and for $\theta_L \rightarrow 0$.

$$\frac{\partial f(x, y)}{\partial y} = \begin{bmatrix} 0 & 1 & 0 & 0 \\ -j_x \frac{1+y_3^2}{[(1+y_1)^2-1-y_3^2]^{\frac{3}{2}}} & 0 & j_x \frac{(1+y_1)y_3}{[(1+y_1)^2-1-y_3^2]^{\frac{3}{2}}} & 0 \\ 0 & 0 & 0 & 1 \\ -j_x \frac{(1+y_1)y_3}{[(1+y_1)^2-1-y_3^2]^{\frac{3}{2}}} & 0 & j_x \frac{(1+y_1)^2-1}{[(1+y_1)^2-1-y_3^2]^{\frac{3}{2}}} & 0 \end{bmatrix} \quad (3.5)$$

Here nonzero elements could be greater and less than one, hence the use of the infinity matrix norm lead to additional difficulties in analysis. Therefore we use Frobenius matrix norm in condition (3.3):

$$\begin{aligned} hb_M \sqrt{2 + j_x^2 \frac{(1+y_3^2)^2 + 2(1+y_1)^2 y_3^2 + ((1+y_1)^2 - 1)^2}{[(1+y_1)^2 - 1 - y_3^2]^{\frac{3}{2}}}} &= \\ &= hb_M \sqrt{2 + j_x^2 \frac{[(1+y_1)^2 + y_3^2]^2 - 2[(1+y_1)^2 - 1 - y_3^2]}{[(1+y_1)^2 - 1 - y_3^2]^{\frac{3}{2}}}} = \\ &= hb_M \sqrt{2 \left(1 - \frac{j_x^2}{\sqrt{(1+y_1)^2 - 1 - y_3^2}} \right) + j_x^2 \frac{[(1+y_1)^2 + y_3^2]^2}{[(1+y_1)^2 - 1 - y_3^2]^{\frac{3}{2}}}} < 1. \end{aligned} \quad (3.6)$$

Revising condition (3.6) in the initial point $(y_1, y_3) = (0, 0)$ we have that expression under the sign of square root is infinite and formally Gear's method of integration cannot converge. This expression also is large if $\theta_L \rightarrow 0$. This explains a bad convergence properties for the numerical experiments with $\sqrt{\theta_L} < 0.01$.

Moreover, even taking small $h > 0$ is not a solution, because a larger number of computational steps increase the rounding error. In the case of the truly stiff (oscilating) problem this local errors compensate each other. In our case the solution is a smooth function posing the error accumulation.

3.4. Steffenson's derivative free self-convergent method. One of the most used derivative free self-convergent methods for solving nonlinear functions and their system is based on the one of a so called Steffenson's estimation. A good discussion of this and other suitable methods could be found in [28].

Temporarily assuming β and arbitrary parameter we introduce iterative function

$$\varphi = x - \frac{\beta f^2(x)}{f(x + \beta f(x)) - f(x)}.$$

Here φ and β are formal parameters. If $|1 + \beta f'(x)| < 1$ and $f(x)/f'(x)$ is small, the introduced function could be more exact than a classical Newton's method. Taking $\beta = -1/f'(x)$ makes this iterative function the third order convergent. Moreover, one can check that

$$f'(x) \approx \frac{\beta f(x)}{f(x + \beta f(x)) - f(x)}.$$

Supposing that β approximates $-1/f'(x)$ we can introduce a formal two step method

$$\begin{cases} x_{i+1} = x_i - \frac{f(x_i)}{\Gamma_i} \\ \Gamma_i = \frac{f(x_i + \beta_i f(x_i)) - f(x_i)}{\beta_i f(x_i)} \\ \beta_i = -\frac{1}{\Gamma_{i-1}} \end{cases} \quad (3.7)$$

To start the process we have to provide two values: x_0 and β_0 . The choice of the starting point is problem dependent, while the choice of β_0 have in immediate impact on the iterations convergence or divergence. Usually we choose β_0 according to the following assumptions:

- (1) If the rough estimation of $f'(x_0)$ can be found, we assume $\beta_0 = -\frac{1}{f'(x_0)}$;
- (2) $\beta_0 = -\frac{f(x_0)}{f(x_0 + f(x_0)) - f(x_0)}$;
- (3) $\beta_0 = \text{sign}(f'(x_0))$.

It is clear that for the “stiff” nonlinear functions with a small local convergence domains the right choice of initial parameter and starting point will be the clue.

The situation becomes even worse for a vector nonlinear functions. In this case an algorithm (3.7) needs to apprximate the Jacobian matrix. Let $x = (x_1, \dots, x_n)$, $f = (f_1(x), \dots, f_n(x))$, $n > 1$ is a problem dimension. Denote

$$t_i^{(k)} = x_i^{(k)} + \beta_{ij}^{(k)} f_j^{(k)}, \quad f_i^{(k)} \triangleq f_i(x^{(k)}),$$

where the upper index is the iteration number, and the lower(s) – the element index. then

$$J_{ij}^{(k)} = J_{ij}(x^{(k)}, t^{(k)}) = \frac{f_i(x_1^{(k)}, \dots, t_j^{(k)}, \dots, x_n^{(k)}) - f_i(x_1^{(k)}, \dots, x_j^{(k)}, \dots, x_n^{(k)})}{t_j^{(k)} - x_j^{(k)}}, \quad (3.8)$$

here $J_{ij}^{(k)}$ is just an extension of standard derivative difference estimation. Denote $H^{(k)} = [J^{(k)}]^{-1}$. Then the generalization of the iterative function 3.7 is defined

$$\begin{cases} x^{(k+1)} = x^{(k)} - H^{(k)} f^{(k)} \\ \beta_{ij}^{(k)} = -H_{ij}^{(k-1)}, \quad i, j = 1 \dots n \\ t_i^{(k)} = x^{(k)} + \sum_{j=1}^n \beta_{ij}^{(k)} f_j^{(k)}, \quad i = 1 \dots n \end{cases} \quad (3.9)$$

An iterative algorithm (3.9) can be easily implemented, but its numerical stability and accuracy depends on the choice of the matrix inversion algorithm and condition number of the Jacobian (3.8). In our case $n = 2$ and we use the explicit computational expressions overriding additional internal computational errors.

3.5. Advanced two-step derivative free self-convergent method. A standard Stefensons estimation discussed above is fast, have a good numerical properties and seems to be enough. But in process of numerical modelling we found it acceptable only if a quantity

$$\sqrt{\theta_L} \gtrsim 0.1 . \quad (3.10)$$

To operate some standard notations, other then φ_L , a_L and θ_L we need to denote a boundary conditions definition domain for system (1.18),(1.19)

$$\mathfrak{D} = \{ \varphi_L, a_L | (1 + \varphi_L)^2 - 1 - a_L^2 > 0 \} , \quad (3.11)$$

$$\bar{\mathfrak{D}} = \{ \varphi_L, a_L | (1 + \varphi_L)^2 - 1 - a_L^2 \geq 0 \} . \quad (3.12)$$

A domain $\mathfrak{D} \subset \bar{\mathfrak{D}}$ where $\bar{\mathfrak{D}}$ domain include all the boundary conditions related to the magnetically insulated diode.

At the moment we investigate the problem of noninsulated diode and the limitation (3.10) is not restrictive. Nevertheless the singularity $\theta_L \approx 0$ makes it impossible the modelling of the border cases and a numerical/analytical investigation of the problem properties in this critical state. As example, assuming $\sqrt{\theta_L} = 0.01$ and varying φ_L we failed to obtain estimations of parameters j_x, β even for $\varphi_L > 12.3$ using second order Gear's implicit and iterative methods, and for $\varphi_L > 10$ using third order Gear's method.

Hence we examined the applicability of the two stage method pseudo-diagonally method, developed by E.V. Dulov. This method description is not published yet, but it was verified in a number of a well known test and practical problems including 3-body problem in the Differential–Algebraic–Equation statement. It demonstrate high numerical stability along with the same speed of computations in this task.

The derivation of the method is not hard but need a lot of attention, this we describe here only the principle.

First of all, we assumed matrix $[\beta_{ij}]$ to be diagonal (a vector of parameters). Hence all the expressions (3.9) are significantly simplified. To obtain a convergence order, higher then second one we need to set some additional conditions for β_i . Since the error of iterative algorithm (3.9) is a $n \times n$ matrix, we can not zero all its elements using only n parameters. So we required diagonal elements to be zero, that gives a condition

$$\beta_i^{(k)} = -\frac{1}{2J_{ii}^{(k)}} . \quad (3.13)$$

The second algorithm step assumes the evaluation of better Jacobian estimation using the data aviable from the pseudo-diagonal version of (3.9) and convex approximation. For simplicity here we provide only scalar form of the vector since in vector generalization is strighforward.

Let

$$\rho(z - x)f'(x) = f(x + \rho(z - x)) - f(x) , \rho \in (0, 1] \quad (3.14)$$

with some additional point z and scalar ρ . This requirement makes the separate use of the convex approximation problematic, and usually it is used as a second stage of some basic iterative algorithm. Hence, denoting

$$f'(x) \approx t(x) = \frac{f(x + \rho(\phi(x) - x)) - f(x)}{\rho(\phi(x) - x)} , \rho \in (0, 1]$$

and supposing that a basic iterative function $\phi(x)$ is at least quadratically convergent, on the basis of (3.7) and (3.14) we obtain a number of different methods with guaranteed convergence orders ≥ 3 , but according to requirements of practical convergence the method of the main interest is a two stage method

$$\begin{aligned}
 \varphi(x) &= x - \frac{\beta f^2(x)}{f(x + \beta f(x)) - f(x)} \\
 t(x) &= \frac{f(x + \rho(\varphi(x) - x)) - f(x)}{\rho(\varphi(x) - x)} \\
 u(x) &= \frac{f(\varphi(x))}{t(x)} \\
 \bar{\varphi}(x) &= \varphi(x) + \frac{u(x)f(\varphi(x))}{f(\varphi(x) - u(x)) - f(\varphi(x))} \\
 \beta &= - \frac{u(x)}{f(\varphi(x) - u(x)) - f(\varphi(x))}
 \end{aligned} \tag{3.15}$$

The merit of this two step method is that at second step we use a better convex β approximation for calculating a resulting point. This two-stage method is more flexible, since we have one additional parameter involved – ρ . A direct analysis of the (3.15) gives that the error term is proportional to

$$\begin{aligned}
 - \frac{15(f^{(2)}(\alpha))^3}{2(f'(\alpha))^5} \left[3(f^{(2)}(\alpha))^2 ((1 - \rho) - \beta f'(\alpha)(\rho + \beta f'(\alpha))) + \right. \\
 \left. + 2f^{(2)}(\alpha)f'(\alpha)(1 + \beta f'(\alpha))(2 + \beta f'(\alpha)) \right] .
 \end{aligned}$$

Here α is a solution point, or the fixed point of the iterative function $\bar{\varphi}(x)$. Substituting optimal $\beta = -\frac{1}{f'(\alpha)}$ in this equation gives zero, but it is easy to see, that the first term in the square brackets depends both from β and ρ , and moreover, the error value involved by this term is minimal for $\rho \equiv 1$. A selection of $\rho = 1$ is meaningless, but it shows that taking ρ close to 1 make two stage algorithm converge more fast. In our numerical experiments we set $\rho = 0.95$. On the other hand, using $\rho \approx 1$ impose smaller integration step and the increased computation time. Hence in the future papers we plan to make a set of additional experiments to find some "optimal" value of the convex approximation parameter ρ .

As a conclusion, this two stage method is twicely time consuming, but it allowed to extend the domain where we can evaluate the critical domain estimations at least for $\varphi_L = 80 \gg 12.5$. The numerical modelling can be further continued, but the already obtained results allow to make some qualified conclusions, provided in sections 4, 5.

3.6. Initial parameter approximation. Any of the introduced algorithms need some initial approximation to be given. It is clear, that we have in general an implicit dependence $g(\varphi_L, a_L, j_x, \beta) = 0$ and one of the most important tasks of our numerical experiments was to build some kind of approximations

$$\begin{aligned}
 j_x &= g_1(\varphi_L, a_L), \\
 \beta &= g_1(\varphi_L, a_L).
 \end{aligned} \tag{3.16}$$

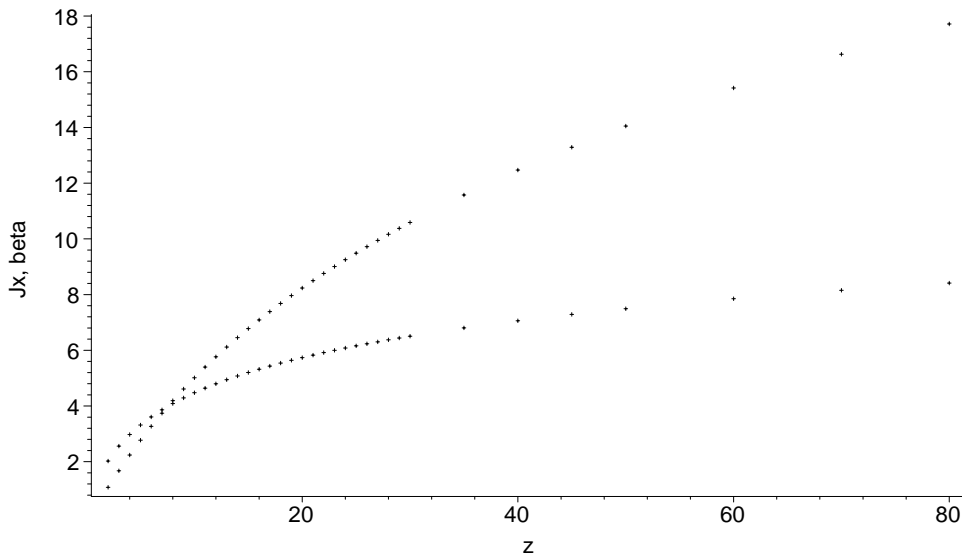


Figure 4.1: j_x, β parameter curves for $\theta_L = 1$.

Here we assume that a reader could easily differ between parameter β as an initial condition of the ODE system and a parameter vector β_0 for the one or two stage pseudo-diagonal derivative free self-convergent method. Without making some good approximation (3.16) we can not give any acceptable apriori estimation. Nevertheless a thousands of numerical runs for different θ_L showed that

$$\beta_0 = \left(-\frac{1}{2\varphi_L}, -\frac{1}{2a_L} \right)$$

is a good one. Hence all our efforts were concentrated on the selection of the proper interpolation/extrapolation functions (3.16).

4. Numerical modelling

Recalling various already made remarks about numerical stability of the solution we have to divide logically all our experiments in to blocks. First of all, we would like to get some information about parameter vector trayectories $p = (j_x, \beta)$ for distances $\theta_L \geq 1$.

4.1. Steady solutions. This paper were aimed only at a preliminary subject study, thus we made only one set of the numerical experiments for $\theta_L = 1$. As we could expect, the errors of integration were smaller for small φ , about 10^{-17} and grow quite fast. They became 10^{-12} only for $\varphi = 80$.

Since the tabulated results are harder to imagine, first we draw them in a pictures for $(z, \sqrt{\theta_L}) = (z, 1)$:

- a) Figure 4.1 assume $z = \varphi_L = 2, \dots, 30, 35, 40, 45, 50, 60, 70, 80$;
- b) Figure 4.2 assume $z = \varphi_L = 0.45, 0.5, 1, 1.25, 1.5, 1.75, 2, 2.5, 3$.

The upper curve correspond to parameter j_x at figure 4.1 and to β at figure 4.2; the lower - to parameter β at figure 4.1 and to j_x at figure 4.2.

This two figures were provided separately for two purposes:

Table 4.1: j_x and β parameter values; $\theta_L = 1$

φ_L	j_x	β
0.45	0.17864868540937	0.30143871969702
0.5	0.20404667713384	0.46737105858652
0.75	0.33864720780410	0.92943647499937
1.0	0.48182248854903	1.23100608581084
1.25	0.62941593031875	1.47230153366985
1.5	0.77957026817339	1.67824795451252
1.75	0.93066609035116	1.86001181745560
2.0	1.08188872124903	2.02350593270070
2.5	1.38117662430921	2.31111775388343
3.0	1.67486318624019	2.55883258218455
4.0	2.23898741598031	2.97439626139971
5.0	2.77064007114640	3.31638912417627
6.0	3.27110218726489	3.60768739672887
7.0	3.74297629896394	3.86166045267669
8.0	4.18905608370126	4.08690609535260
9.0	4.61195944040519	4.28931729704208
10.0	5.01456658887901	4.47437644974364
11.0	5.39796579347806	4.64282381562656
12.0	5.76436673093679	4.79821194565616
13.0	6.11532511808196	4.94242313464426
14.0	6.45219825697198	5.07695868731263
15.0	6.77617430735118	5.20303567114342
16.0	7.08829752910593	5.32165465243329
17.0	7.38948962373869	5.43364831404905
18.0	7.68056762187826	5.53971710886889
19.0	7.96225883273576	5.64045590084838
20.0	8.23521334223292	5.73637420356129
21.0	8.50001448436446	5.82791178241683
22.0	8.75718764266414	5.91545084189829
23.0	9.00720767619584	5.99932565877550
24.0	9.25093999416217	6.08028976674331
25.0	9.48792823466859	6.15769586302146
26.0	9.71894291624990	6.23222252722460
27.0	9.94431109427948	6.30407601910147
28.0	10.1643328203516	6.37344121169832
29.0	10.3792840656884	6.44048444952802
30.0	10.5896457275944	6.50556737370551
35.0	11.5757743817479	6.80172674079113
40.0	12.4704804229310	7.05966669855577
45.0	13.2907790793456	7.28812444567524
50.0	14.0492090856849	7.49314749947562
60.0	15.4164568319502	7.84921457963099
70.0	16.6269099012908	8.15164335637439
80.0	17.7149884119297	8.41407321211649

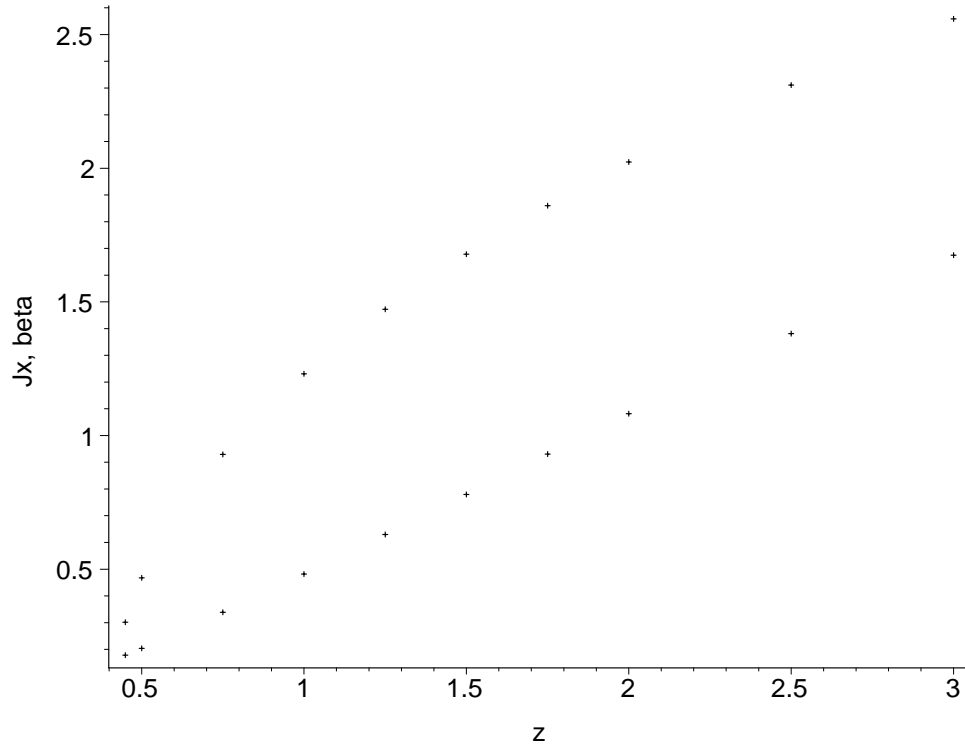


Figure 4.2: j_x, β parameter curves for $\theta_L = 1$.

- a) β trajectory seems to keep the same character over the whole interval. This character is likely to be $(ax)^b$, $b < 1$;
- b) j_x trajectory character is different for $z \leq 2.5$ and $z > 2.5$. The right branch is the convex function, but at the left the sign of the $j_x^{(2)}(\varphi_L, a_L)$ is changed. The corresponding approximation curve could be similar to $a \frac{x^b}{x^c + d}$, for example.

REMARK 4.1. To ensure the correctness of the above results, we applied formulae (1.23), (1.24) to some of the numerically evaluated solution curves with a proper parameter vectors. The exact numerical differences vary, keeping 10^{-7} coincidence order that is sufficient for verification.

4.2. Bifurcating solutions. Considering $\theta_L < 1$ we are expected the similar results to be obtained. Also we wanted to revise our suggestion, that parameter vector (j_x, β) will bifurcate. And this suggestion was numerically approved. So, hereinafter we call

$$\{(\varphi_L, a_L) \in \mathfrak{D}_B | \theta_L < 1\}$$

a bifurcation domain. The reader will find some corresponding results nearby in the subsection. We found that there exist many bifurcation branches, but all of them lie behind the supreme one. Hence one of the main goals for this set of numerical experiments were to evaluate the curves like 4.1, 4.2 and revise, if they are similar.

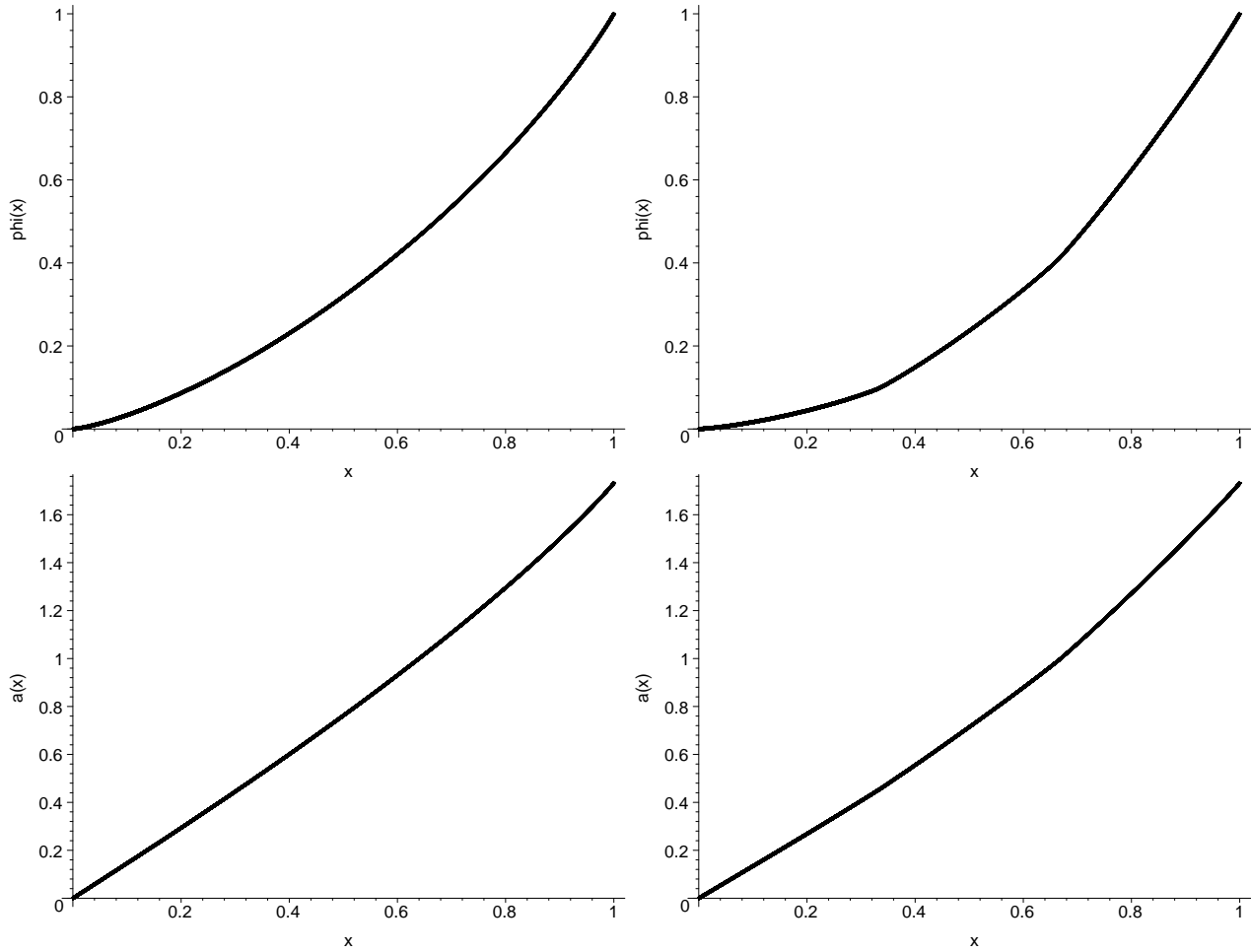


Figure 4.3: Solution trajectories in bifurcation domain: $\sqrt{\theta_L} = 0.01$. $\varphi(x)$ on the top, $a(x)$ at bottom. Each column corresponds to different parameter sets.

Here we present the solution trajectories overall (figure 4.3) obtained for $\sqrt{\theta_L} = 0.01$, $p = (1.0, 1.73202194)$. The upper drawings there are the trajectories of the solution $\varphi(x)$; drawings at bottom — $a(x)$.

The right column represent a solution for parameter vector

$$(0.362038663209651, 1.44751573598728).$$

The left column represent a solution for parameter vector

$$(0.120963091314551, 1.33267484682958).$$

Additionally here we put the numerical estimations for $\varphi(x)$ and $a(x)$ derivatives at final point $x = 1$:

$$\varphi'(1) = 2.34183172164059, \quad a'(1) = 2.75180985565606$$

$$\varphi'(1) = 2.40105767552903, \quad a'(1) = 2.74567972060528$$

As we could expect, the second parameter vector with smaller j_x makes the $\varphi(x)$ curve more convex.

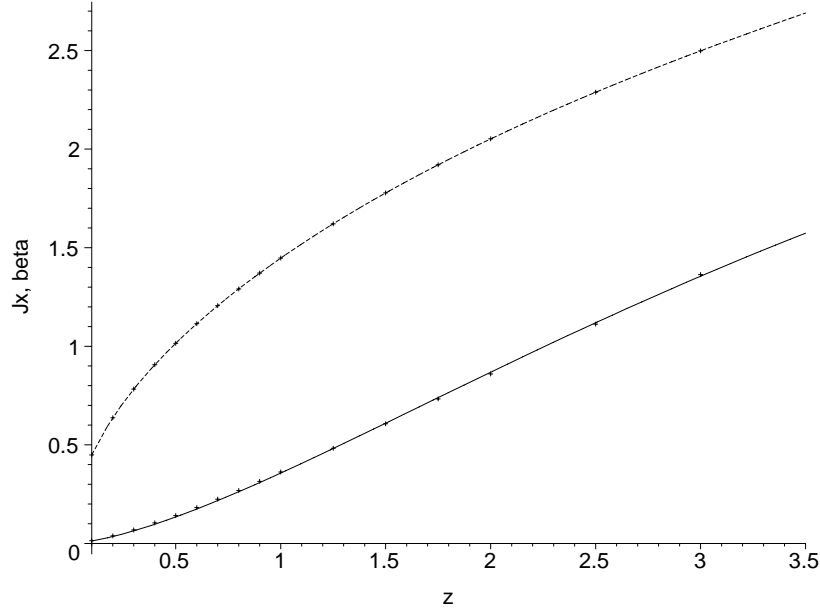


Figure 4.4: j_x, β parameter curves for $\sqrt{\theta_L} = 0.01$. j_x approximation is given by solid line; β approximation is marked by dashed line.

Backing to the discussion of the \mathfrak{D}_B , we present figure 4.4 as a set of different j_x evaluated for $\varphi \in [0, 3]$, $\theta_L = 0.01$. A reader can compare them with a similar steady parameter solution at figure 4.2. Figure 4.4 also contain a curves for the possible parameter approximations

$$j_x(z) \approx 4.176975526 \frac{z^{1.49}}{z^{1.49} + 10.7} \text{ — solid line;}$$

$$\begin{aligned} \beta^2(z) \approx & 0.00682158147416591417z^4 - \\ & - 0.0586365860652600102z^3 + 0.138861698566226766z^2 + \\ & + 2.00763692651626435z - 0.0006674981435 \text{ — dash line.} \end{aligned}$$

The overall picture 4.5 is given for $z = \varphi \in [0, 80]$ and should be referred with figure 4.1. Here

$$j_x(z) \approx 3.239692865 \frac{z^{1.55}}{z^{1.17} + 12} \text{ — solid line;}$$

$$\begin{aligned} \beta^2(z) \approx & -0.290786558759896149 \cdot 10^{-5}z^4 + \\ & + 0.000581674456932978232z^3 - 0.0450013788913051077z^2 + \\ & + 2.17534075031773888z + 0.02819502302 \text{ — dash line.} \end{aligned}$$

All the coefficients for j_x approximation functions, except the first one, were estimated manually just to illustrate their partial coincidence. Coefficients of the β approximation were obtained by the standard least square method implemented in *Maple* package.

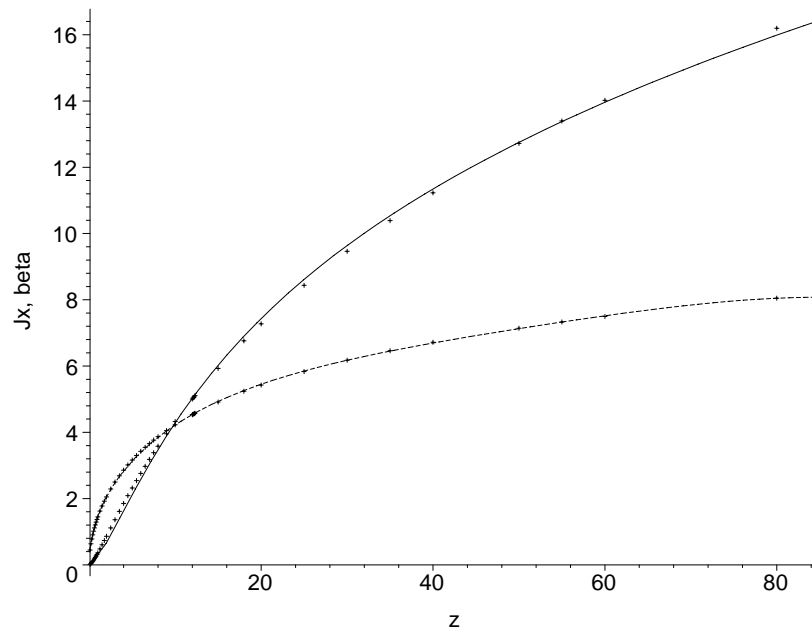


Figure 4.5: j_x, β parameter curves for $\sqrt{\theta_L} = 0.01$. j_x approximation is given by solid line; β approximation is marked by dashed line.

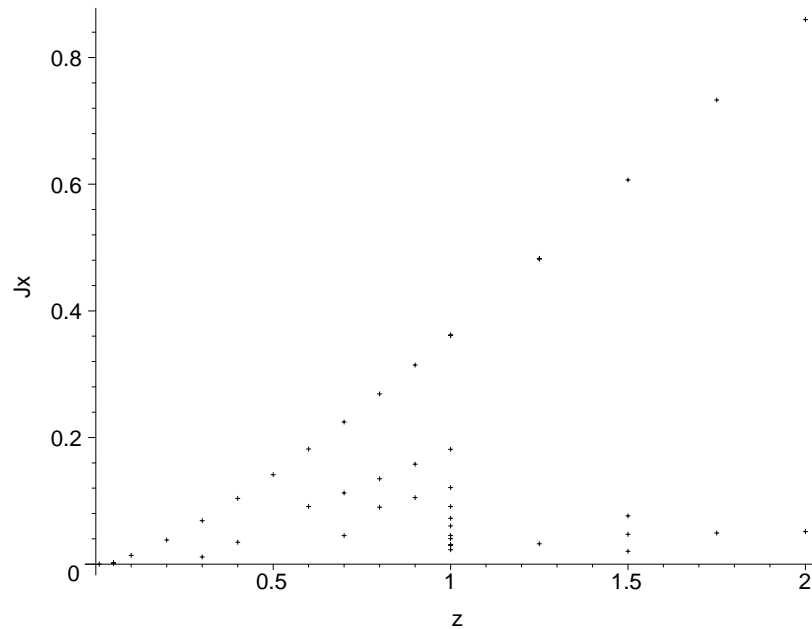


Figure 4.6: Some j_x parameter sets for $\sqrt{\theta_L} = 0.01$.

The last figures 4.6,4.7 represent (only partially) the elaborated array of parameter vectors for $\varphi \in [0, 2]$, $\sqrt{\theta_L} = 0.01$.

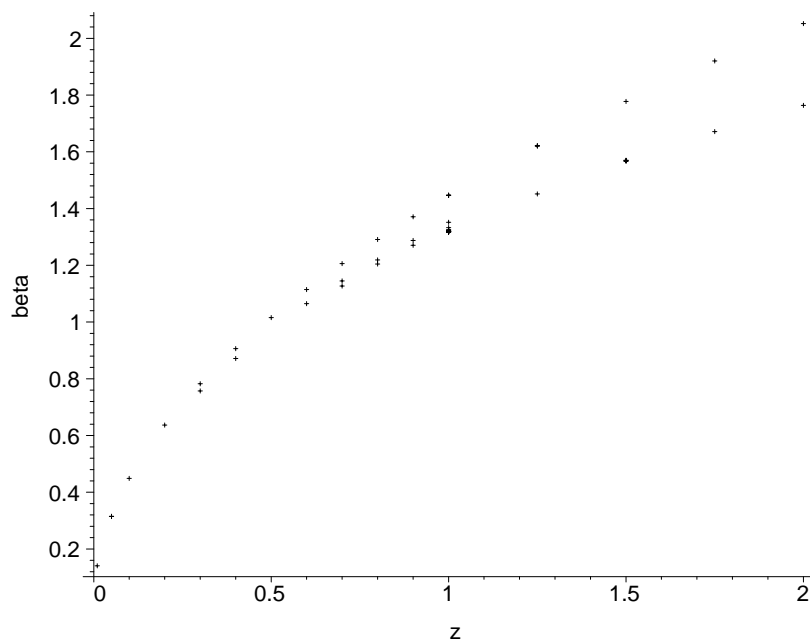


Figure 4.7: Some β parameter sets for $\sqrt{\theta_L} = 0.01$.

The numerical results visualized in figures 4.6 and 4.7 are of a great practical importance. As we can see, the set of bifurcating parameters make a quite dense bundle for the self-magnetic cathode potential β , while the current density j_x vary from 0 to certain supreme value. Keeping in mind the principles underlying the vacuum diode and the descriptions of the current fluctuations factor made in introduction, we see, that even a small change of an external magnetic field destroy the dynamic balance of the emitted and falling back electrons, as well as characteristics of electro-magnetic potential barrier. Then the discrete current impulse carried by electron vary. Since it takes a lot of computation time to trace each possible trayectory, the figures like 4.6, 4.7 will be enchanced in further research publications. Using only numerical modelling we cannot verify what kind of bifurcation behaviour we have. Differently speaking, this figures show that we have a multiple branches, but we are not shure if they are infinite and if there is a hard dependency from θ_L quantity.

The mathematical treatment of this problem require the special methods of singular bifurcation analysis [21],[24], while according to physical effects some of the parameter trayectories are too close to differ between them while modelling such an effects in physical space due to natural fluctuations of the applied potential and external magnetic field.

Additionally we provide a table 4.2 containing (only for example) the pairs of parameter vectors evaluated for the same $\varphi_L = 1$ and different a_L inside \mathfrak{D}_B .

Paying attention to the first five rows one can see that some of the bifurcation trayectories are very close and the change of θ_L produces a smooth change of parameters (j_x, β) .

REMARK 4.2. To verify the properties of the bifurcating by analogy with remark 4.1 we have substituted some of the trayectory numbers into the (1.23),(1.24) relations. And as it was expected, this relations are fullfilled only for the "upper" bifurcating solution, giving the

Table 4.2: A set of bifurcational parameter vectors, $\varphi_L = 1$.

a_L	$\sqrt{\theta_L}$	j_x	β
1.731	0.060324	0.365663946368995 0.354300520581914	1.44952586822602 1.43968411868464
1.73	0.082615	0.367876733994073 0.348835570011430	1.45034495903031 1.43389667379108
1.728	0.118389	0.371320851204937 0.338903268894778	1.45114820399346 1.42330549498369
1.7265	0.138556	0.373472399881449 0.331879535436268	1.45138649703371 1.41583361639305
1.725	0.156125	0.375401344169635 0.325056868543785	1.45143842210438 1.40862852384825
1.71	0.275500	0.389380241218800 0.232421083855372	1.44758087738484 1.33470731432593

same 10^{-5} – 10^{-7} error coincidence value. The slightly higher error level is explained by a high numerical sensitivity of computational method, while we keep the same integration step size.

Being applied to the bifurcating solutions which parameters j_x and β are smaller than "upper" ones, we got the coincidence errors of order 10^{-3} and higher. Definitely speaking, the relations (1.23), (1.24) are describing only steady-state solutions for $\theta_L \geq 1$ and supreme bifurcating solutions.

5. Partial conclusions

One of the main conclusions to be made is the fact that a statement of limit problem (1.18)–(1.22) does not comply with a Child-Langmuir regime that a current density j_x is saturated in the case of non-insulated or nearly-insulated diode. Moreover, with a respect to figures 4.1, 4.5 and the rough numerical approximations made, the current density j_x will infinitely grow if the voltage applied to the diode also grows. On the other hand, the experimental data show that j_x grow faster for non-insulated diode than for a nearly-insulated one. This could be seen as an preliminar numerical proof that a Child-Langmuir regime could be achieved only in magnetically insulated diode.

The second conclusion refers to the nearly-insulated diode. As it was shown in illustrations at bifurcation part of article and provided there comments, the discovered properties described by a limit problem in mathematical statement fully comply with their physical expectations described in introduction section. Jointly with a first conclusion made, it characterises the obtained limit model as a reliable one, that complies with the physical processes, underlying the thermo-vacuum diode with a plane cathode and anode.

The third conclusion is the consistency of the proposed numerical methods for the problem (1.18)–(1.22). The only, but the serious lack raised by the model singularity is the difficulty in translating the dimensionless model into the physical space, because the investigated boundary conditions are far away of the voltage and magnetic field values used either in semiconductor and home device manufacturing, or in the modelling of the high energy devices.

Things to do

The started research has some interacting, but very specific things to do:

- For better analysis of steady solutions parameter dependencies we have to elaborate two arrays of data (φ_L, a_L, j_x) and (φ_L, a_L, β) . This data triplets represent some 3D surfaces giving an intermediate presentation of the parametric dependences (j_x, β) ;
- To make some asymptotic conclusions on the properties of the "upper" bifurcation parameter trajectories we need to elaborate the sets of data arrays (φ_L, a_L, j_x) and (φ_L, a_L, β) for $\theta_L \rightarrow 0$;
- Using the above data and some known analytical dependences we have to construct some completely defined approximation functions describing parameter behaviour;
- Since the limit problem provide only the rough solution estimation for the general problem, we have to develop a software, resolving original system (1.11)–(1.17) for φ^ε , a^ε , and involved parameters;
- The dimensionless problem statements have to be transformed into their physical analogs with proper numerical modelling software;
- Using the accumulated knowledge base and developed software we will be able to resolve and make a numerical experiments for the magnetically insulated diode both in dimensionless and physical model spaces.

Acknowledgment

We kindly thanks our colleague Natalia Andrianova for her valuable support and useful discussions.

References

- [1] N. Ben Abdallah, The Child-Langmuir regime for electron transport in a plasma including a background of positive ions, *Math. Models Methods Appl. Sci.*, 4, (1994), pp. 409-438.
- [2] N. Ben Abdallah, P. Degond, F. M'ehats, The Child-Langmuir asymptotics for magnetized flows.
- [3] N. Ben Abdallah, P. Degond, F. M'ehats, Mathematical models of magnetic insulation, *Asymptotic Analysis*, Vol. 20, (1999), pp. 97-132.
- [4] N. Ben Abdallah, P. Degond et A. Yamnahakki, The Child-Langmuir law as a model for electron transport in semiconductors, *Solid-State Electronics*, Vol. 39, No. 5, (1996), pp. 737-744.
- [5] P. J. Christenson and Y. Y. Lau, Transition to turbulence in a crossed-field gap, *Phys. Plasmas*, 1 (12), (1994), pp. 3725-3727.
- [6] R.M. Corless, L.F. Shampine, Initial Value Problems for ODEs in Problem Solving Environments, *J. Comp. Appl. Math*, Vol. 125, No. 1-2, (2000), pp. 31-40.
- [7] J.M. Creedon, Relativistic Brillouin flow in the high ν/γ diode, *J. Appl. Phys.*, Vol. 46, No. 7, (1975), pp. 2946-2955.
- [8] J.M. Creedon, Magnetic cutoff in high-current diodes, *J. Appl. Phys.*, Vol. 48, No. 3, (1977), pp. 1070-1077.
- [9] P. Degond, S. Jaffard, F. Poupaud, P.-A. Raviart, The Child-Langmuir Asymptotics of the Vlasov-Poisson Equation for Cylindrically or Spherically Symmetric Diodes. Parts 1 and 2, *Math. Methods Appl. Sci.*, 19, (1996), pp. 287-312 and pp. 313-340.
- [10] P. Degond, P.-A. Raviart, An asymptotic analysis for the one-dimensional Vlasov-Poisson system, *Asymptotic Anal.*, 4, (1991), pp. 187-214.

- [11] P. Degond, P.-A. Raviart, On a penalization of the Child-Langmuir emission condition for the one-dimensional Vlasov-Poisson equation, *Asymptotic Anal.*, 6, (1992), pp. 1-27.
- [12] M. Di Capua, Magnetic Insulation, *IEEE Trans. Plas. Sci.*, Vol. PS-11, No. 3, (1983), pp. 205-215.
- [13] C.W. Gear, Numerical Initial Value Problems in Ordinary Differential Equations, *Prentice-Hall*, (1971).
- [14] E. Hairer, G. Wanner, Solving Ordinary Differential Equations II: Stiff and Differential-Algebraic Problems, *Springer*, (1996).
- [15] A.W. Hull, The effect of a uniform magnetic field on the motion of electrons between coaxial cylinders, *Phys. Rev.*, 18, (1921), pp. 31-57.
- [16] O. Kelly, Shot noise in a Diode, *El. manuscript*, (1999), <http://www.maths.tcd.ie/~olly/shot.pdf>, p. 11.
- [17] I. Langmuir, K.T. Compton, Electrical discharges in Gases : Part II, Fundamental Phenomena in Electrical Discharges, *Rev. Mod. Phys.*, 3, (1931), pp. 191-257.
- [18] Y.Y. Lau, P.J. Christenson, D. Chernin, Limiting current in a crossed-field gap, *Phys. Fluids B.*, Vol. 5, No. 12, (1993), pp. 4486-4489.
- [19] R.V. Lovelace, E. Ott, Theory of magnetic insulation, *Phys. Fluids*, Vol. 17, No. 6, (1974), pp. 1263-1268.
- [20] F. M'ehats, The Child-Langmuir asymptotics applied to the bipolar diode, to appear.
- [21] V.K. Melnikov, On the stability of the center for time-periodic perturbations, *Transl. Mosc. Math. Soc.*, Vol. 12, (1963), pp. 1-57.
- [22] E. Ott, R.V. Lovelace, Magnetic insulation and microwave generation, *App. Phys. Lett.*, Vol. 27, No. 7, (1975), pp. 378-380.
- [23] F. Poupaud, Boundary value problems for the stationary Vlasov-Maxwell system, *Forum Mathematicum*, 4, (1992), pp. 499-527.
- [24] C. Robinson, Horseshoes for autonomous Hamiltonian systems using the Melnikov integral, *Ergodic Th.Dyn.Sys.*, Vol. 8, (1988), pp. 395-409.
- [25] A. Ron, A.A. Mondelli, N. Rostoker, Equilibria for magnetic insulation, *IEEE Trans. Plas. Sci.*, Vol. PS-1, No. 4, (1973), pp. 85-93.
- [26] A.V. Sinityn, Positive solutions of nonlinear singular boundary-value problem of magnetic insulation, *Int. Rep. of Universidad Nacional de Colombia*, No. 84, (2002), p. 16.
- [27] J.A. Swegle, Nonexistence of quasilaminar equilibria in cylindrical magnetically insulated lines, *Phys. Fluids*, Vol. 25, No. 7, (1982), pp. 1282-1285.
- [28] J.F. Traub, Iterative Methods For The Solution Of Equations, *Chelsea Pub. Comp.*, New York, (1982).